**„Babeş-Bolyai” University, Faculty of Physics**

**Cluj-Napoca**

**Interdisciplinary Research Institute on Bio-Nano-Sciences**

**Paula Ildikó Fodor (Riti)**

# Effect of calcium and magnesium addition on the bioactivity of silicate glasses prepared by different sol-gel routes

**PhD Thesis Summary**

**Scientific supervisor:**
**Prof. Dr. Viorica Simon**

**2014**

**Babeş-Bolyai University, Faculty of Physics**

# Effect of calcium and magnesium addition on the bioactivity of silicate glasses prepared by different sol-gel routes

**PhD Thesis Summary**

PhD candidate:
**Paula Ildikó Fodor (Riti)**

Scientific supervisor:
**Prof. Dr. Viorica Simon**

**Cluj-Napoca, 2014**

***** Keywords:*** *Sol–gel, gelation time, silica, bioactive glass, alkaline earth oxides (CaO, MgO)*

# Table of Contents

# INTRODUCTION

The aim was to synthesise silicate bioactive glasses modified with calcium oxide and magnesium oxide prepared via sol-gel method following the acid catalysed and the quick alkali mediated routes and to characterise the obtained samples with repsect to their structure, morphology and texture, and finally to study their bioactivity.

Both acid catalysed and quick alkali-mediated sol-gel routes ensure accessible way to obtain new bioactive materials [1] which can be used for bone repair or regeneration [2]. The capacity of these materials to form a bond with a living tissue is named bioactivity [3] which ability takes place through the development of a biological apatite layer when those materials are immersed in physiological solutions [3, 4].

Magnesium is an important element in the family of bioactive glasses because it is involved in over 300 chemical reactions and can activate phagocytosis and regulate active calcium transport [5]. Therefore the magnesium ions play a significant role in the qualitative changes of bone matrix, determining the fragility of bones and, on the other hand, the depletion of magnesium adversely affects all stages of skeletal metabolism, causing cessation of bone growth [6, 7].

The sol-gel route [8] is a chemical synthesis technique based on inorganic polymerisation reactions of metal alkoxide and metal salt precursors which permits the production of amorphous and polycrystalline materials with specific properties, such as uniformity, high-purity grade and large surface area [9]. The “quick-set” process was developed [10] to obtain rapid gelation by the adjustment of the acid sol’s pH with dilute ammonium hydroxide that reduces at room temperature, the gelation time from a few days to a few minutes.

The thesis is divided into three chapters, followed by general conclusions, list of scientific papers and list of international conferences. The first chapter presents the literature aspect of bioactive glasses, describing the role of magnesium in the prepared glasses and also incorporates background information about acid catalysed and quickly gelled sol- gel synthesis route and bioactivity assay. The second chapter gives a description of the characterisation techniques used for material analysis. The third chapter is the main part of this research work and describes the obtained experimental results and the discussions of them.

## 1. Effect of calcium and magnesium addition to pure silica investigated for $75SiO_2 \cdot 25CaO$, $64.5SiO_2 \cdot 21.5CaO \cdot 14MgO$ bioactive glasses

### 1.1 Samples preparation

The compositions of the prepared glasses in mol % are: pure $SiO_2$, $100 \cdot SiO_2$ (referred hereinafter as Si_A) synthesised following the acid catalysed route, and Si_Q as quickly prepared using the acid catalysed base condensed method, $75 \cdot SiO_2$ - $25 \cdot CaO$ (SiCa_A and SiCa_Q), $64.5 \cdot SiO_2$ - $21.5 \cdot CaO$ - $14 \cdot MgO$ (SiCaMg_A and SiCaMg_Q).

The reagents used were $SiC_8H_{20}O_4$ (*TEOS*) - precursor for $SiO_2$, $Ca(NO_3)_2 \cdot 4(H_2O)$ (calcium nitrate tetrahydrate) - precursor for CaO, $Mg(NO_3)_2 \cdot 6(H_2O)$ (magnesium nitrate hexahydrate) - precursor for MgO.

To obtain $100 \cdot SiO_2$ samples, TEOS, distilled water and nitric acid were mixed and the mixture was allowed to react for 30 min under continuous stirring for the acid hydrolysis of TEOS. Then half of the solution was left for gelation (Si_A) and to the other half ammonia solution was added drop wise under continuous steering for quick gelation (Si_Q). In case of multicomponent glasses the appropriate amounts of reagents, dissolved previously in distilled water, were added to the 1.5 pH TEOS solution under continuous steering. Following the same procedures as for the Si_A and Si_Q syntheses, SiCa_A, SiCa_Q, SiCaMg_A and SiCaMg_Q systems were obtained. The samples prepared by A route were gelled at room temperature and had different gelation times, and the solvent was removed from the resulted gels by drying at 110 °C for 24 hours in a drying oven.

### 1.2 Sample characterization by thermal analysis

To see the thermal evolution, the samples were analysed with a Shimadzu differential thermal analyser DTG-60H witch simultaneously measures TG and DTA. These results for the as prepared (dried) six samples are shown in Figure 1.1.

The DTA curves reveal an initial endothermic process around 100 ºC for all the samples, accompanied by weight loss, as observed in the TG runs. These events can be attributed to loss of residual water and ethanol. This weight loss is more gradual in the case of acid catalysed samples and occurs over a range of temperatures up to 450 ºC. The second part of the slope corresponds to the loss of organics and desorption of chemically absorbed water (exothermic event around 270 ºC). In case of the quickly gelled samples the water and organic residues removal is well evidenced in the TG curves by the two weight loss steps in 100 - 450 ºC temperature region. There are no other thermal events visible in case of the two single component samples (Si_A, Si_Q).

The TG curves of the multicomponent glasses present another weight loss step in the 450-600 ºC temperature range associated with endothermic events in the DTA and accounted to the decomposition of nitrates ($NO_3^-$) and ammonia ($NH_4$) residues, respectively.

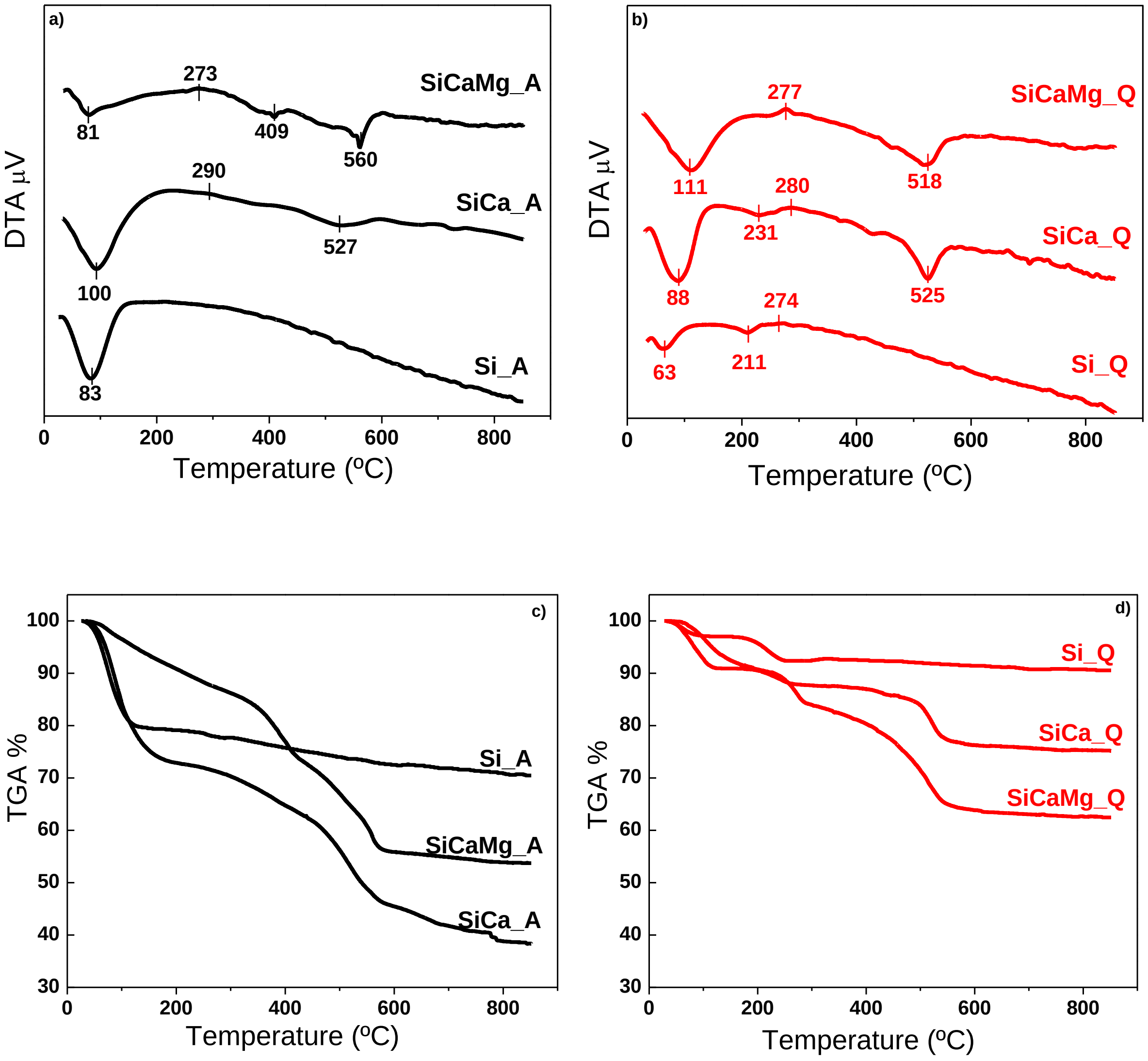

***Figure 1.1*** *DTA / TG curves for* $100\cdot SiO_2$, $75SiO_2\cdot 25CaO$ *and* $64.5SiO_2\cdot 21.5CaO\cdot 14MgO$ *prepared by A route (a,c) and by Q route (b, d) as prepared samples.*

The DTA/TG results indicate that all synthesis residues are completely eliminated up to 600 ºC temperature. According to the obtained results the stabilization temperature was established at 600 ºC for all the samples for one hour.

## 1.3 Structural characterisation by X-ray diffraction

The structure of the thermally stabilised samples at 600 ºC was investigated using X-ray diffraction analysis to assess the crystallinity of the glasses and the results are presented in Figure 1.2.

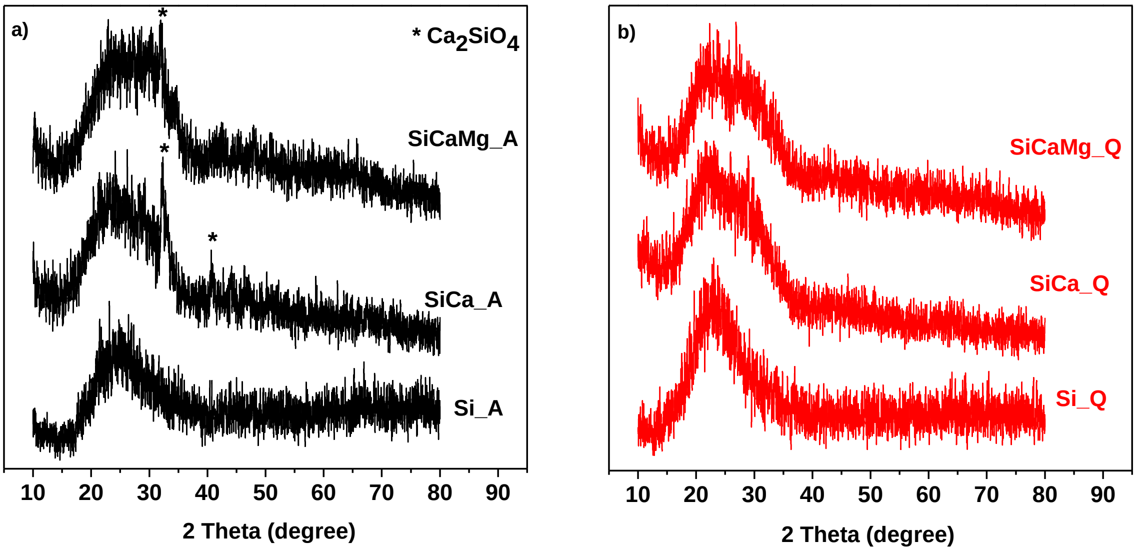

***Figure 1.2*** *XRD patterns of the thermal treated samples prepared by A route (a) and by Q route (b)*

Both acid catalysed (A) and quickly gelled (Q) sample sets present a predominant amorphous structure with a shoulder between 15- 35 º in 2 theta range. The SiCa_A sample thermally treated at 600 ºC presents an incipient crystalline phase, identified as $Ca_2SiO_4$ (dicalcium silicate, JCPDS pdf No. 20-0237) that was reported by Liu et al. to have excellent bioactivity [11].

## 1.4 Structural characterisation by FTIR spectroscopy

The IR absorption spectra of the six silicate matrices (Figure 1.3) present the specific three main bands assigned to different vibration modes of the Si–O–Si bonds. The band located at ~465 $cm^{-1}$ is assigned to rocking motion of the bridging oxygen atoms perpendicularly to the Si–O–Si plane also known as transverse-optical $TO_1$ mode [12]. At ~805 $cm^{-1}$ is observed a weak band due to transverse-optical symmetric stretching of the O atom along a line bisecting the Si–O–Si angle ($TO_2$) [12]. The spectra are dominated by a strong and large band with the maximum at ~1100 $cm^{-1}$ assigned to antisymmetric stretching mode of Si–O–Si group [13], involving motions back and forth of the oxygen atom along a line parallel to the Si–Si axis (TO$_3$) [12].

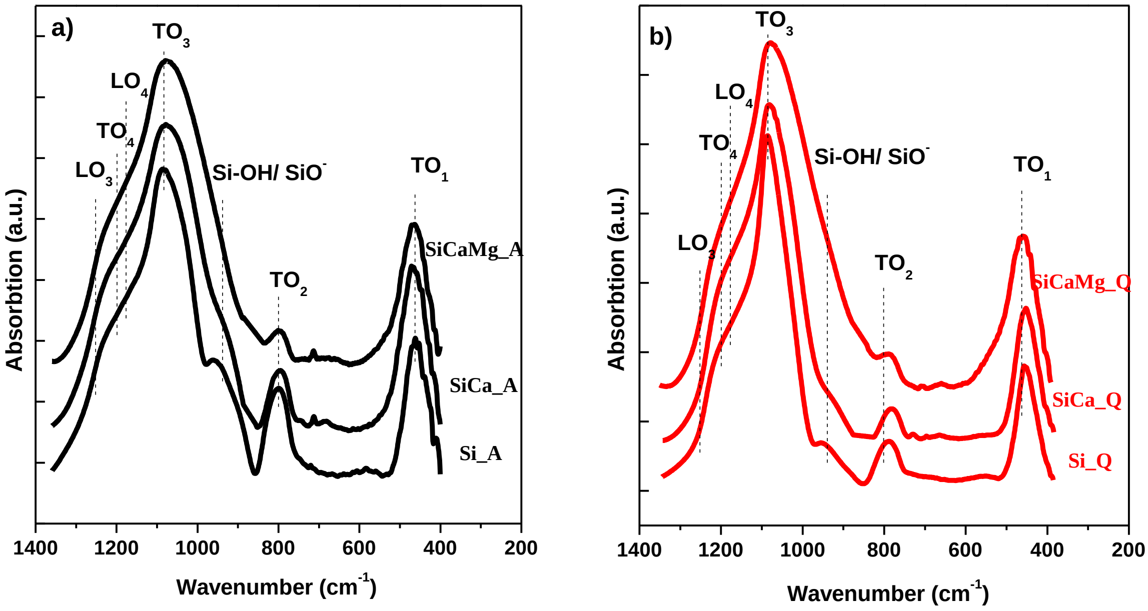

***Figure 1.3*** *FTIR spectra of the thermal treated samples prepared by A route (a) and by Q route (b).*

The shoulder centred near 940–960 cm$^{-1}$, very pronounced in the FTIR spectra of Si_A sol-gel glass, is due to Si–OH stretching vibrations [12]. The absorption band given by the stretching vibrations of Si–OH groups are known to decrease in intensity due to matrix densification with increasing of thermal treatment temperature and time [12]. If comparing the intensities of absorption signals corresponding to Si-OH vibrations from the two FTIR spectra of the single component matrices prepared by the two different sol-gel routes it can be observed that densification is higher in the case of acid catalysed base condensed Q route.

The shoulder at ~1250 cm$^{-1}$ is due to the longitudinal-optic splitting of LO$_3$ vibration modes [12]. The presence of the ~1250 cm$^{-1}$ shoulder (LO$_3$) is important in sol-gel derived materials and is specific to porous silica [12, 13]. The intensity of LO$_3$ mode is known to increase with porosity due to the scattering of the IR radiation within the pores [12]. Taking into consideration the contribution of LO$_3$ vibration band, the Si_Q sample seems to have the highest porosity. This shoulder may be considered [14] as a convolution of three different vibrations: LO$_3$, TO$_4$ and LO$_4$, at around 1254, 1200 and 1170 cm$^{-1}$, respectively. The other two components of this shoulder LO$_4$ - TO$_4$ known as disorder –induced vibration modes, are correlated with an increased disorder in the microstructure [12]. The presence of this vibration modes is evident in the case of multicomponent silicate glasses prepared by both A and Q preparation routes, with a higher intensity for the Q samples. By introducing CaO, MgO, and CaO with MgO, respectively, the IR spectra reveal also other changes. The band at ~ 465 $cm^{-1}$ is broadened toward higher wavenumbers, while the band at ∼800 $cm^{-1}$ undergoes a gradual decrease and shifts slightly to lower wavenumbers, phenomena also observed by Kalampounias [13]. In the high-frequency region, the intensity of the band at ~950 $cm^{-1}$ increases relative to that of the band located at 1100 $cm^{-1}$. In alkali silicate glasses, the ~950 $cm^{-1}$ band is assigned to Si-O-NBO stretching vibrations with one non-bridging oxygen (NBO) per $SiO_4$ tetrahedron ($Q^3$ units) [15]. It can be also observed for Q samples that by introducing of MgO in the calcium silicate matrix the absorption band centered at 1100 $cm^{-1}$ is broadened towards lower values. This broadening may be due to Si-O-2NBO stretching vibrations in $Q^2$ units, specific for silicate matrices with high modifier content [13], denoting that in this case magnesium behaves as a network modifier even if is present in a relatively high concentration (14 mol%).

This behaviour is not so evident for the same composition prepared by A route but there are still visible differences and in this case part of magnesium oxide may act as a network intermediate oxide and enter into the silicate network as $MgO_4$ tetrahedral units [16]. McMillan [17] found that Dietzel's ionic field strength (I) of network modifier cations are less than 5 $Å^{-2}$, but $Mg^{2+}$ with I =4.73 $Å^{-2}$ is considered to fall on the boundary between a network modifier and an intermediate oxide [18]. Kalampounias reports [13] that the extent of network depolymerisation in a sol-gel derived porous glass is higher than in a melted derived bulk one of similar composition. In this work, it can be observed that network depolymerisation is higher for the samples prepared following the Q route than for the samples of the same composition prepared following the A route.

### 1.5 BET surface area and pore volume measurements

Specific surface area and pore volume results show that comparing the A route samples with the Q route ones, the Q sample series have a higher pore volume, and the total surface area is also higher excepting the Si_Q sample as shows Figure 1.4.

The specific surface areas for the samples with only one alkaline earth oxide incorporated in the glass matrix are higher than the specific surface areas of the samples containing both CaO and MgO obtained by the two preparation routes. Furthermore the specific surface area of the magnesium containing sample prepared by Q route has a similar value as the only calcium containing sample prepared by A method. These aspects lead us to the conclusion that the Q route permits the incorporation of Mg as network modifier beside calcium without affecting the specific surface area as in the A route prepared samples.

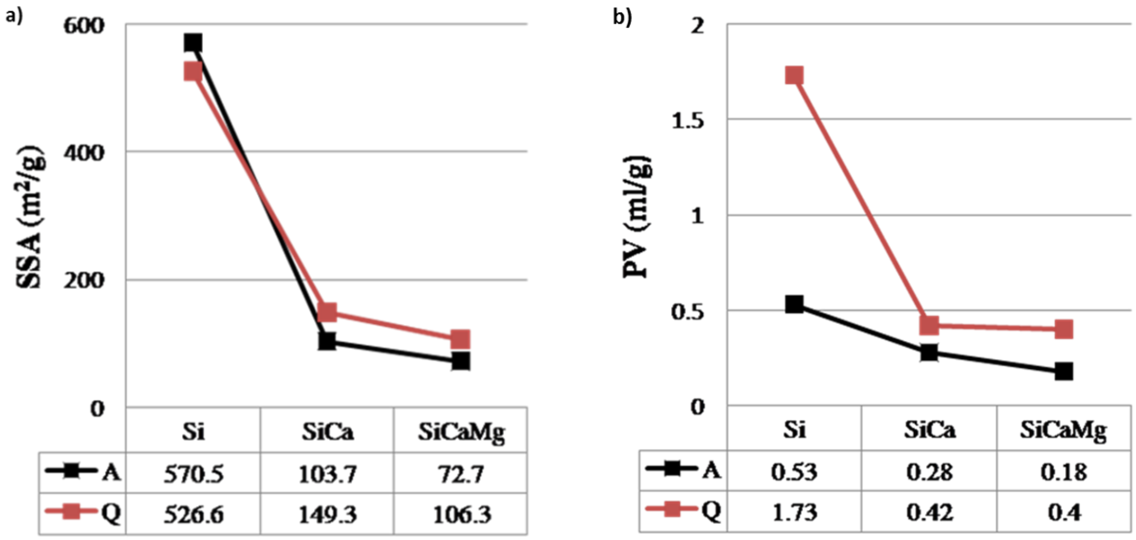

***Figure 1.4*** *Specific surface area (a) and pore volume (b) of the 100·SiO$_2$, 75·SiO$_2$ - 25·CaO and 64.5·SiO$_2$ - 21.5·CaO - 14·MgO thermal treated samples prepared by A and Q sol-gel route.*

## 1.6 Bioactivity studies

In order to investigate the samples bioactivity, 40 mg of glass powders were soaked in 10 ml SBF at 37 ºC under static conditions. The immersion time was 1, 3, 7 and 14 days and after these periods we studied hydroxyapatite (HA) formation by XRD, FTIR SEM and EDS analysis in comparison with their non-immersed counter parts.

### 1.6.1 XRD measurements after SBF immersion

The XRD patterns recorded from the dried samples are shown in figure 1.5. The diffractograms show that hydroxyapatite (HA) formation on the samples surface is evident in case of SiCa_A, SiCa_Q and SiCaMg_Q glasses. One day and 3 days of SBF soaking are insufficient time intervals for HA formation, but specific peaks for CaCO$_3$ were observed in case of two component samples. After 7 days of immersion in SBF occurs the peak characteristic for HA. After 14 days of immersion HA crystals are evidenced for both alkaline earth oxide (CaO, MgO) containing quickly gelled samples, moreover the magnesium containing quickly gelled sample’s diffractogram presents the most intense HA characteristic peaks from all the immersed samples. In terms of the samples prepared by A sol-gel method only the calcium containing silicate matrix presents in vitro apatite crystalline phase formation, this phase formation being inhibited by the presence of magnesium following this kind of preparation route.

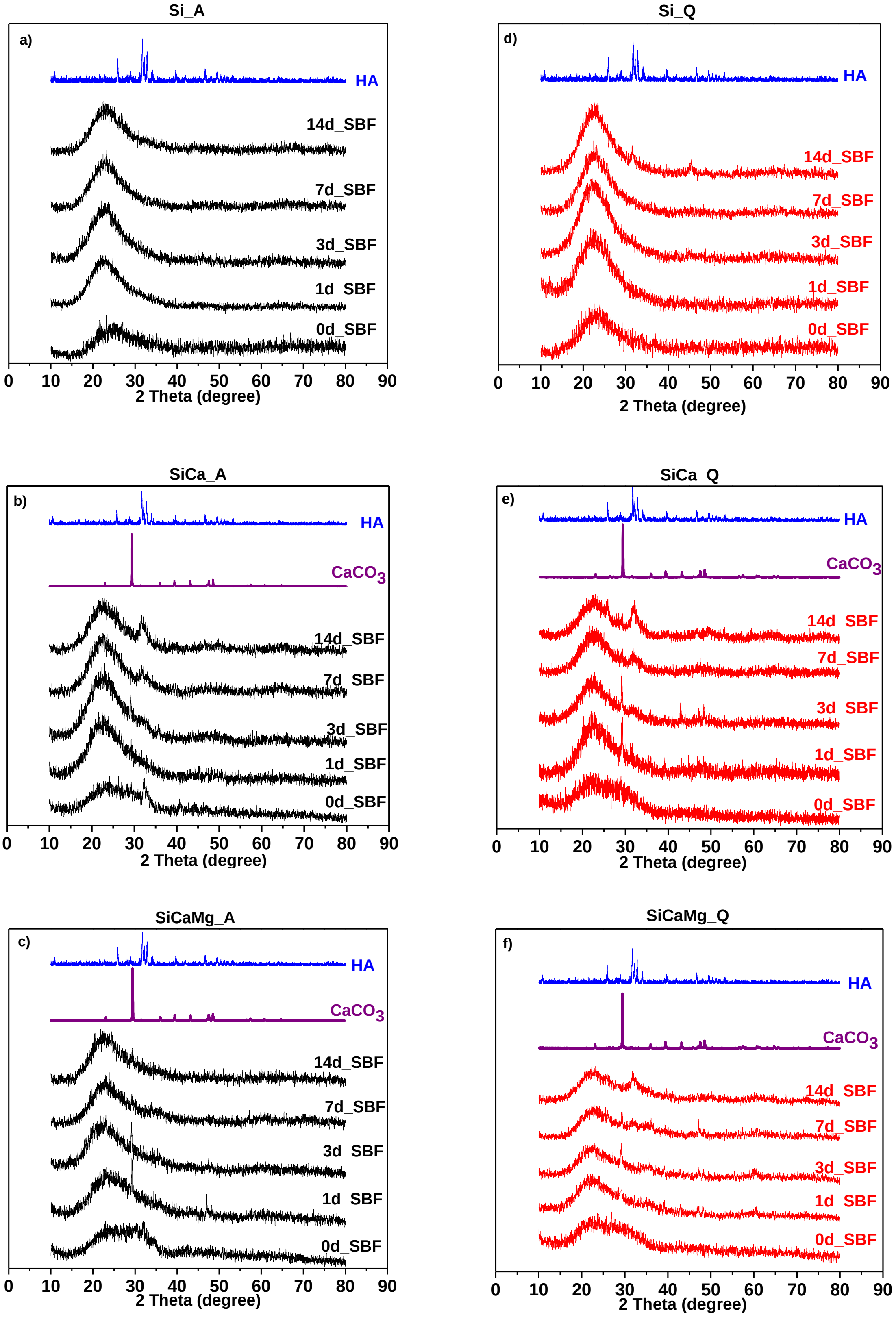

***Figure 1.5*** *XRD patterns for A prepared (a, b, c) and Q prepared (d, e, f) samples after 1, 3, 7 and 14 days immersion in SBF.*

### 1.6.2 FTIR measurements after SBF immersion

The FTIR spectra recorded after SBF incubation (Figure 1.6) support the results obtained from X-ray diffraction analysis. The presence of HA is confirmed by the appearance in the spectra of the absorption bands around 570 cm-$^1$ and 604 cm-$^1$, respectively, doublet characteristic for the vibration of [$PO_4$] units from crystalline HA phase [4, 19].

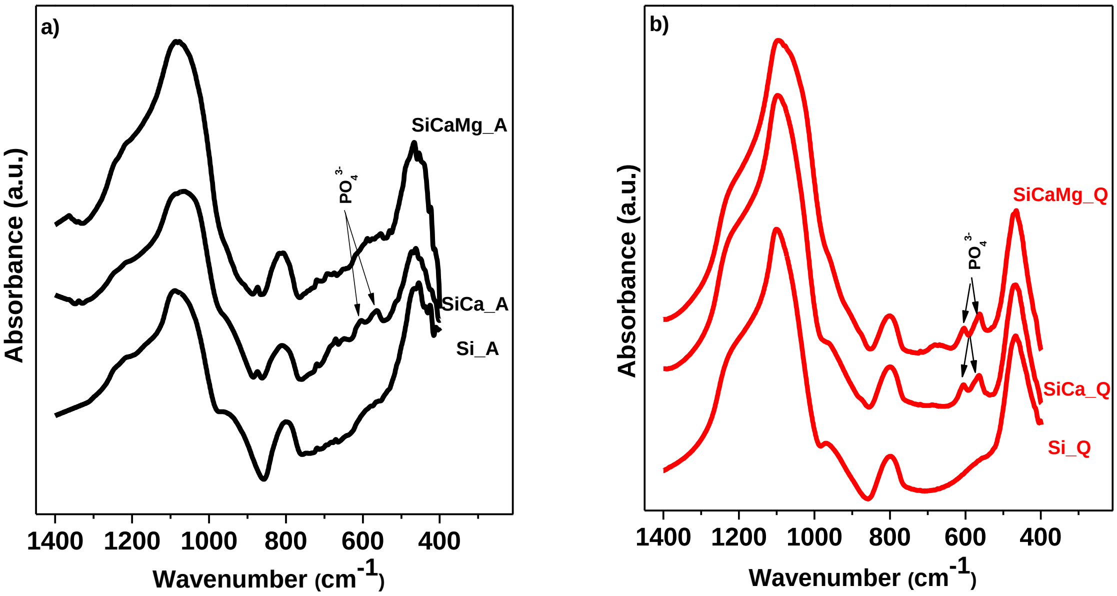

***Figure 1.6*** *FTIR spectra of the 100·$SiO_2$, 75$SiO_2$·25CaO and 64.5$SiO_2$·21.5CaO·14MgO samples prepared by acid route (a) and by quick gelation method (b) after 14 days of SBF immersion.*

### 1.6.3 SEM/ EDS measurements after SBF immersion

Scanning electron microscopy measurements (Figure 1.7 a, b, c) reinforce the above mentioned bioactivity of the three glasses SiCa_A, SiCa_Q and SiCaMg_Q. This observation is also supported by the EDS analysis (Figure 1.7 d, e, f), where the phosphorus appears in the elemental analysis and has significant values in atomic %. The highest phosphorus value (16 atomic %) presents the SiCaMg_Q glass.

Some of the obtained results were published in a specialized ISI journal [20].

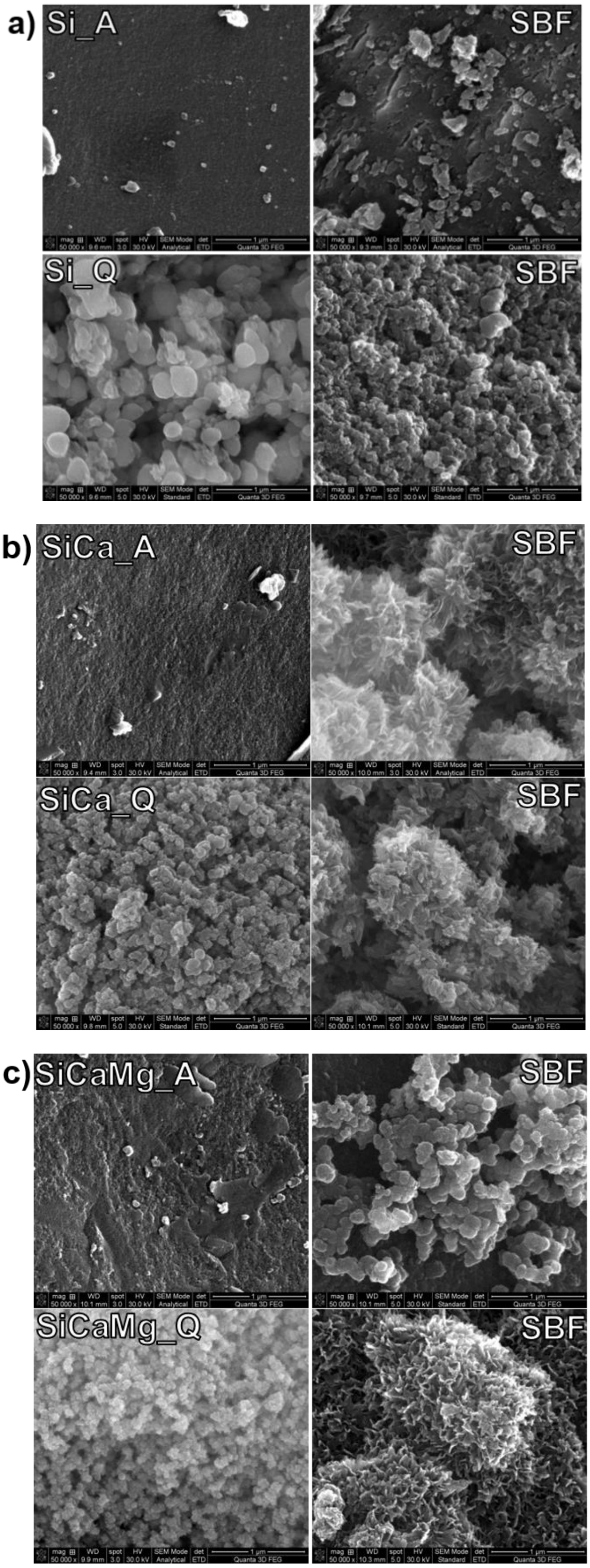

| | Si_A | Si_A_SBF | Si_Q | Si_Q_SBF |
|---|---|---|---|---|
| O | 53,5 | 46,3 | 55,3 | 50,1 |
| Si | 46 | 52,9 | 44,7 | 48,3 |
| Ca | - | 0,1 | - | 0,7 |
| P | - | 0,7 | - | 0,9 |

| | SiCa_A | SiCa_A_SBF | SiCa_Q | SiCa_Q_SBF |
|---|---|---|---|---|
| O | 53,3 | 43,5 | 54,7 | 44,3 |
| Si | 35,6 | 33,1 | 37 | 45 |
| Ca | 11,1 | 11 | 8,3 | 4,8 |
| P | - | 12,2 | - | 6 |

| | SiCaMg_A | SiCaMg_A_SBF | SiCaMg_Q | SiCaMg_Q_SBF |
|---|---|---|---|---|
| O | 37,3 | 47,5 | 48,4 | 45,4 |
| Si | 8,5 | 44,8 | 32,4 | 19,2 |
| Ca | - | 1,6 | 14,1 | 17,1 |
| P | - | 3,3 | - | 16 |
| Mg | 7,6 | 2,8 | 5,1 | 2,3 |

***Figure 1.7*** *SEM images of the* $100 \cdot SiO_2$*,* $75SiO_2 \cdot 25CaO$ *and* $64.5SiO_2 \cdot 21.5CaO \cdot 14MgO$ *samples prepared by A and Q route prior to SBF immersion and after immersion (a, b, c) and EDS analysis of the mentioned samples (d, e, f).*

## 1.7 Conclusions

Silica glasses ($SiO_2$, $SiO_2$-CaO and $SiO_2$-CaO-MgO) modified by alkaline earth oxides (CaO, MgO) were prepared following both slowly gelled and quickly gelled routes. According to the thermal history of the samples evaluated with DTA, all the samples were heat treated at 600ºC for one hour. After the stabilization process, all the samples have predominant amorphous character, but $Ca_2SiO_4$ crystals were evidenced in 75•$SiO_2$•25CaO sample prepared via acid catalysed process as evidenced by the diffraction line at ~ $2\theta=29^{o}$.

After applying the heat treatment the specific surface area and the pore volume are enhanced, the quickly prepared samples have higher porosity then their acid catalysed counterpart samples. The specific surface area and pore volume are higher for the samples with only one alkaline earth oxide incorporated in the glass matrix. Specific peaks for apatite phase appear after 7 days of immersion in the XRD patterns. The apatite phase is evidenced by the absorption bands recorded around 570 $cm^{-1}$ and 604 $cm^{-1}$ in the FTIR spectra specific for the phosphate groups. These results are also supported SEM images and by EDS analysis recorded from the 14 days immersed samples.

The most bioactive among from all the investigated samples proved the sample prepared by quick acid catalysed base condensed sol-gel route containing calcium and magnesium too. Furthermore the quick acid catalysed base condensed sol-gel method permits the incorporation of MgO and by keeping the desired porosity and bioactivity of magnesium free calcosilicate bioactive glass prepared by acid mediated route. Ergo the magnesium oxide was demonstrated to improve the bioactivity of glasses if prepared by alkali mediated sol-gel route, and inhibits this property in case of acid catalysed route preparation.

## 2. Effect of calcium and magnesium addition to pure silica investigated for $70SiO_2 \cdot 30CaO$, $70SiO_2 \cdot 20CaO \cdot 10MgO$, $70SiO_2 \cdot 15CaO \cdot 15MgO$, $70SiO_2 \cdot 10CaO \cdot 20MgO$ and $70SiO_2 \cdot 30MgO$ bioactive glasses

### 2.1 Sample preparation

For investigate the magnesium influence on the properties of the glasses were chosen other compositions for new calcium silicate glass preparation with different MgO concentrations.

In this case the CaO concentration in mol % was gradually replaced with MgO in the calcium – silicate matrix. The systems were obtained via sol – gel method following the acid catalysed route and the quick alkali mediated route. The preparation routes schematic diagram is presented in Figure 2.1.

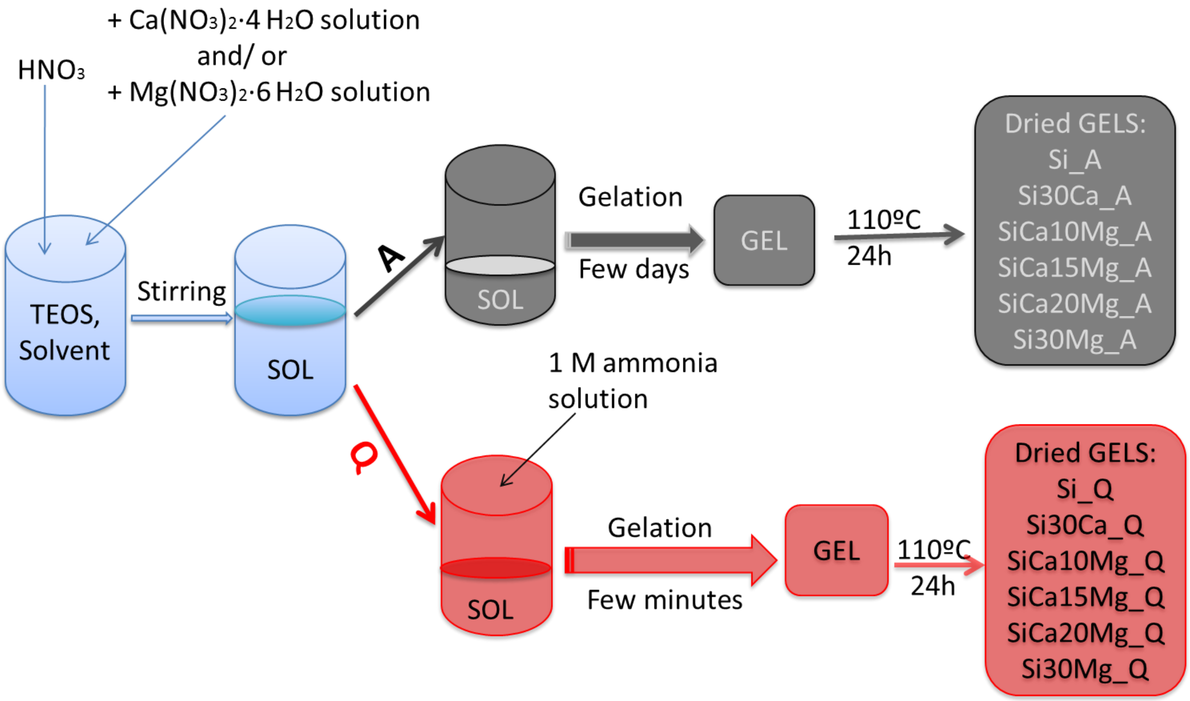

***Figure 2.1*** *Schematic chart for the preparation of glasses using the sol-gel method with two ways: the acid route (A) and the quick alkali mediated (Q) route.*

Following the procedure as mentioned in the first part ten systems were obtained: Si30Ca_A, Si30Ca_Q, SiCa10Mg_A, SiCa10Mg_Q, SiCa15Mg_A, SiCa15Mg_Q, SiCa20Mg_A, SiCa20Mg_Q, Si30Mg_A, and Si30Mg_Q. The ammonia amount added in the pH ~ 2 solution for obtain the multicomponent samples via quick gelation sol – gel method was the following: 4 ml 1 M ammonia for Si30Ca_Q and Si30Mg_Q, 7.5 ml 1 M ammonia for SiCa10Mg_Q, 11 ml 1 M ammonia for SiCa15Mg_Q, and 12 ml 1 M ammonia for

SiCa20Mg_Q. The samples prepared by A route had different gelation times: 2 days Si_A, 5 days Si30Ca_A, 5 days SiCa10Mg_A, 4 days SiCa15Mg_A, 6 days SiCa20Mg_A, and 7 days for Si30Mg_A. In order to remove the solvent entrapped in the systems all the samples, after gelation, were dried for 24 hours at 110 °C in a drying oven.

### 2.2 Sample characterization by thermal analysis

For thermal behaviour characterisation and for thermal treatment temperature evaluation the as prepared samples were investigated by means of Shimadzu differential thermal analyser DTG-60H wich simultaneously measures TGA and DTA and the obtained results are presented in Figures 2.2, 2.3 and 2.4.

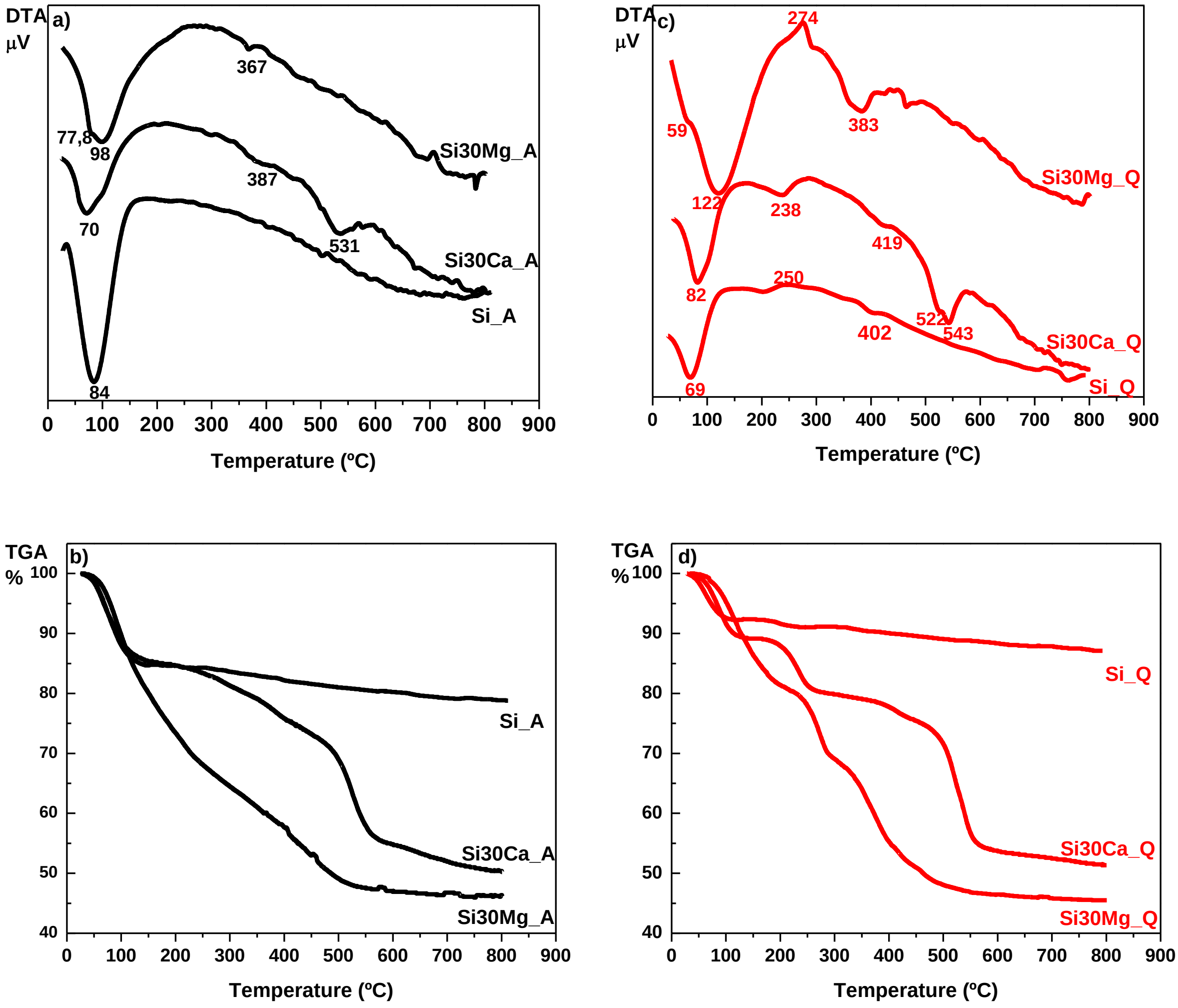

***Figure 2.2*** *DTA/TG results for the 100·$SiO_2$, 70·$SiO_2$·30·CaO, and 70·$SiO_2$·30·MgO samples prepare by A route (a, b) and by Q route (c, d).*

An initial endothermic process is evidenced at all the samples around 100 ºC which can be attributed to loss of residual water and ethanol and it is associated with a weight loss in TG. At the Si_A sample the endothermic event occurs at 84 ºC and the weight loss is 20% from the total mass (Figure 2.2 a, b). In case of the Si_Q sample are two more events. The second is an exothermic event at 250 ºC which is assigned to the combustion of ethylic radicals. The third endothermic phenomenon at ~ 400 ºC associated with weight loss (2%) in TG, probably is due to the elimination of the remaining organic groups. The TG curve of the silicate glasses modified by CaO respectively MgO shows a substantial weight loss in the 200- 550 ºC temperature region corresponding to the endothermic DTA peak, indicating that a large portion of water and organic materials are being removed and the metal nitrate decomposes.

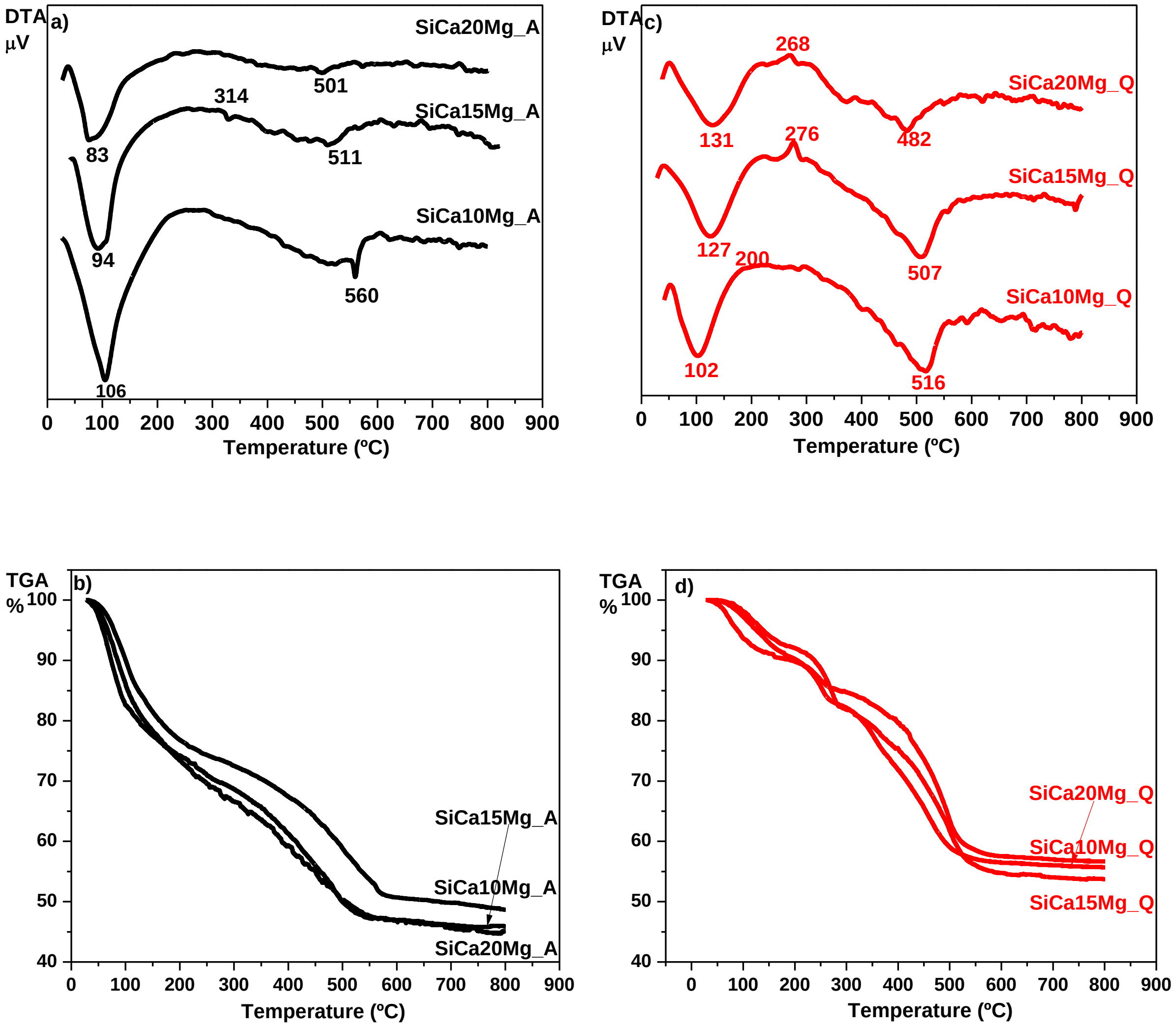

**Figure 2.3** *DTA/TG results for the* $70 \cdot SiO_2 \cdot 20 \cdot CaO \cdot 10 \cdot MgO$, $70 \cdot SiO_2 \cdot 15 \cdot CaO \cdot 15 \cdot MgO$ *and* $70 \cdot SiO_2 \cdot 10 \cdot CaO \cdot 20 \cdot MgO$ *prepare by A route (a, b) and by Q route (c, d).*

The calcium nitrate decomposes slowly, in three steps, and this event finished at ~550 ºC in case of Q gelled sample (30% from total mass loss) and at 530 ºC for A prepared ones (~30% weight loss) [21]. At magnesium containing samples an exothermic peak centred at around 274°C on the DTA curve of Q gelled sample, which is attributed to desorption of chemically adsorbed water. The endothermic process observed at MgO containing samples occurs at around 367 ºC (A prepared sample) and 383 ºC (Q prepared sample) with a weight loss of 20% respective 15% attributed to the loss of nitrates used in the sol preparation.

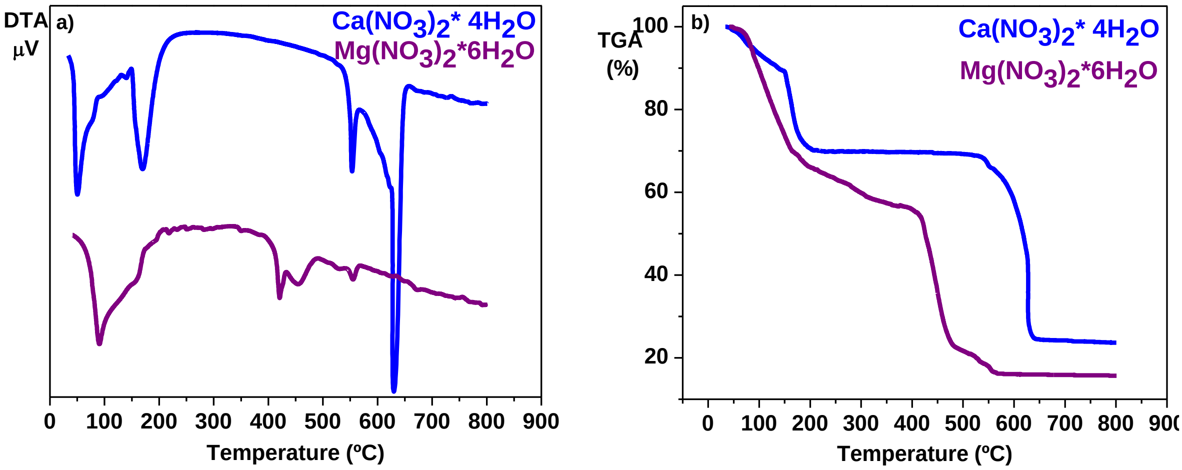

***Figure 2.4*** *DTA (a) and TG (b) results for* $Ca(NO_3)_2*4H_2O$ *and for* $Mg(NO_3)_2* 6H_2O$

The metal nitrates, precursors used for CaO and MgO, DTA and TG results are separately presented in Figure 2.4 for comparison.

In case of three component samples (containing CaO and MgO to, Figure 2.3) were found specific events for both calcium and magnesium as well. After the first endothermic event around 100 ºC due to the elimination of water and ethanol accompanied with weight loss in TG begins the metal nitrate decomposition.

In this case the metal nitrate (Ca and Mg) decomposition occurs simultaneously, and is influenced by the amount of calcium nitrate or magnesium nitrate used in the glass preparation. The event ended at lower temperature in case of SiCa20Mg_A at 501 ºC and at 482 ºC for SiCa20Mg_Q and at higher temperatures for SiCa10Mg_A (560 ºC) respectively SiCa10Mg_Q (516 ºC). The phenomena is accompanied with a weight loss in TG curves, the A prepared samples having higher total mass loss. The exothermic event around 276 ºC (SiCa15Mg_Q) and 268 ºC (SiCa20Mg_Q) present for higher Mg content samples can be attributed to desorption of chemically adsorbed water.

According to the obtained results the metal nitrate elimination process ended before 600 ºC. Hence the stabilization temperature was established at 600 ºC for all the samples for one hour as the previous sample sets.

## 2.3 Structural characterisation by X- ray diffraction

The structure of the samples after applying the 600 ºC one hour thermal treatment was characterised using X-ray diffraction analysis as shows Figure 2.5.

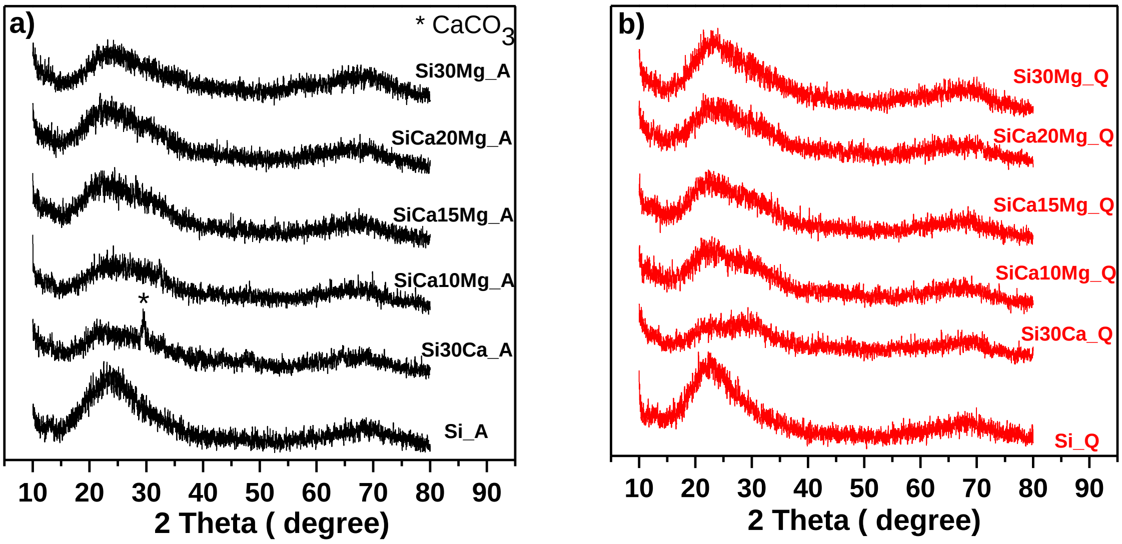

***Figure 2.5*** *XRD patterns of A (a) and Q (b) prepared the 100·$SiO_2$, 70·$SiO_2$·30·CaO, 70·$SiO_2$·20·CaO ·10·MgO, 70·$SiO_2$·15·CaO ·15·MgO, 70·$SiO_2$·10·CaO ·20·MgO and 70·$SiO_2$ ·30·MgO samples.*

The diffractograms recorded from the samples after calcination at 600 ºC / 1h shows that all the samples present predominant amorphous character regardless the preparation route (acid or quick alkali mediated) excepting the Si30Ca_A glass. The Si30Ca_A sample present an incipient crystalline phase in 2 theta range, identified as $CaCO_3$ (calcite, RRUFF ID: R040070.1).

## 2.4 Structural characterisation by FTIR spectroscopy

For this reason the samples were measured in absorption mode in 4000 to 400 cm$^{-1}$ spectral domain with a spectral resolution of 4 cm$^{-1}$ using KBr pellet technique and the results are presented in Figure 2.6.

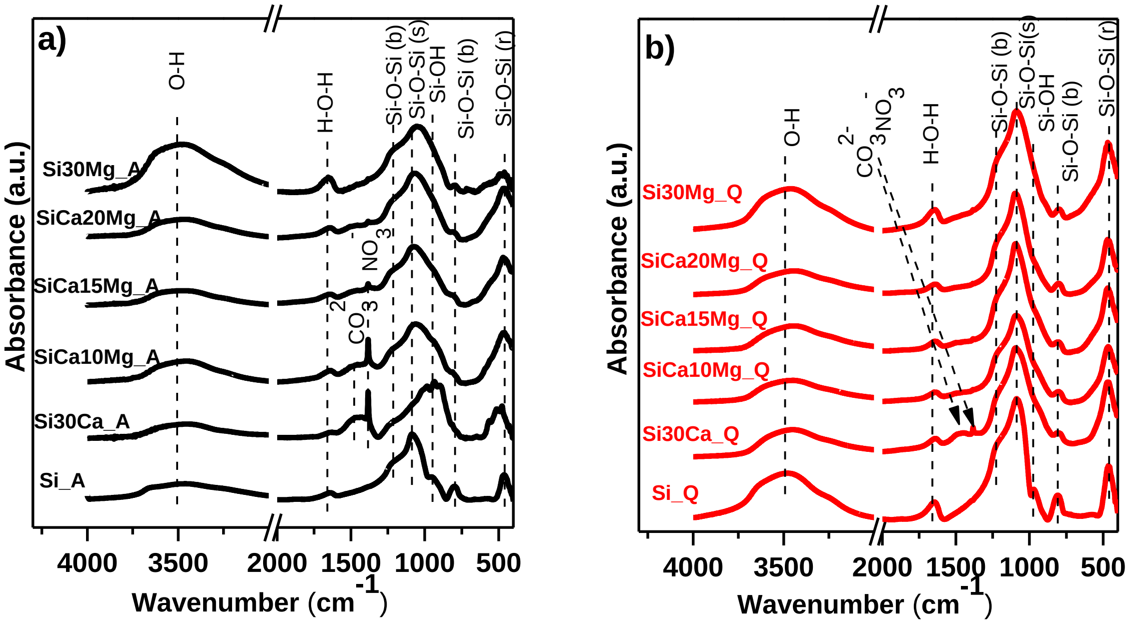

***Figure 2.6** FTIR spectra of the 100·$SiO_2$, 70·$SiO_2$·30·CaO, 70·$SiO_2$·20·CaO ·10·MgO, 70·$SiO_2$·15·CaO ·15·MgO, 70·$SiO_2$·10·CaO ·20·MgO and 70·$SiO_2$·30·MgO samples prepare by A (a) and by Q (b) route.*

The carbonate presence on the Si30Ca_A, SiCa10Mg_A and Si30Ca_Q samples surface is evidenced also by FTIR spectra. Nitrate residues are as well observed in case of mentioned three samples from these results. Specific vibrations of silicate groups are evidenced for all samples and no major structural changes were observed. Samples prepared by quick gelation method, but also by the acid prepared once the Si – O – Si vibration band from 1100 cm$^{-1}$ [22] is broader being the modifier effect on the silica network. With increasing the magnesium concentration in the prepared samples this band becomes broader.

### 2.5 BET surface area and pore volume measurements

Surface area and pore volume results are presented in Table 2.1 which were achieved from the 600 ºC / 1h thermal treated samples.

The first observation from surface area and pore volume results the quickly prepared sample set present higher porosity as the acid catalysed obtained ones. In the same time it can remarked that the surface area increases with the increasing the amount of MgO for A and Q prepared samples excepting Si30Mg_Q.

Table 2.1 Specific surface area and pore volume of the samples prepared by A and by Q sol-gel route.

| **Concentration** | **SSA Acid ($m^2/g$)** | **SSA Quick ($m^2/g$)** | **PV Acid (ml/g)** | **PV Quick (ml/g)** |
|---|---|---|---|---|
| **Si** | 231.7836 | 579.4702 | 0.53 | 0.8074 |
| **Si30Ca** | 46.5182 | 77.27998 | 0.2185 | 0.3533 |
| **SiCa10Mg** | 119.3431 | 150.6818 | 0.3237 | 0.6436 |
| **SiCa15Mg** | 102.7523 | 160.0858 | 0.305 | 0.7886 |
| **SiCa20Mg** | 135.3191 | 153.719 | 0.4346 | 0.782 |
| **Si30Mg** | 103.8618 | 163.0705 | 0.2475 | 0.6058 |

In order to remove the carbonates and nitrates observed in X-ray diffractograms and IR spectra it were chosen other heat treatment values to determine the optimal one. For this six samples (Si_A, Si_Q, Si30Ca_A, Si30Ca_Q, Si30Mg_A and Si30Mg_Q) were subjected to the following thermal treatments: 400 ºC for 6 hours, 600 ºC for 1 hour, 600 ºC for 6 hours and 800 ºC for 1 hour.

### 2.6 TG measurements of thermal treated calcium silicate and magnesium silicate samples

Thermo gravimetric analyses were performed on the calcium silicate and magnesium silicate samples after calcination at various temperatures as shows Figure 2.7.

The first endothermic process observed at approximately 100 ºC associated with the decomposition of water is accompanied by weight loss. With increasing the stabilization temperature the mass loss in this region of temperature decreases. In case of quickly gelled samples this weight loss is smaller compared with the acid catalysed slowly gelled ones even if for preparation of the Q samples more water was added with dilute ammonia.

The phenomenon probably is caused by the sintering phenomena that take place with pH change from acid to slightly basic one for rapid gelation process [10]. With the addition of calcium and magnesium in the silica network the metal nitrate decomposition steps are well defined in case of quickly gelled samples. The total decomposition of nitrates and any other undesired preparation residues is confirmed by the absence of weight loss at 600 ºC for the stabilised samples. The slight mass loss observed in the 800_1h stabilised samples is attributed to structural densification [23].

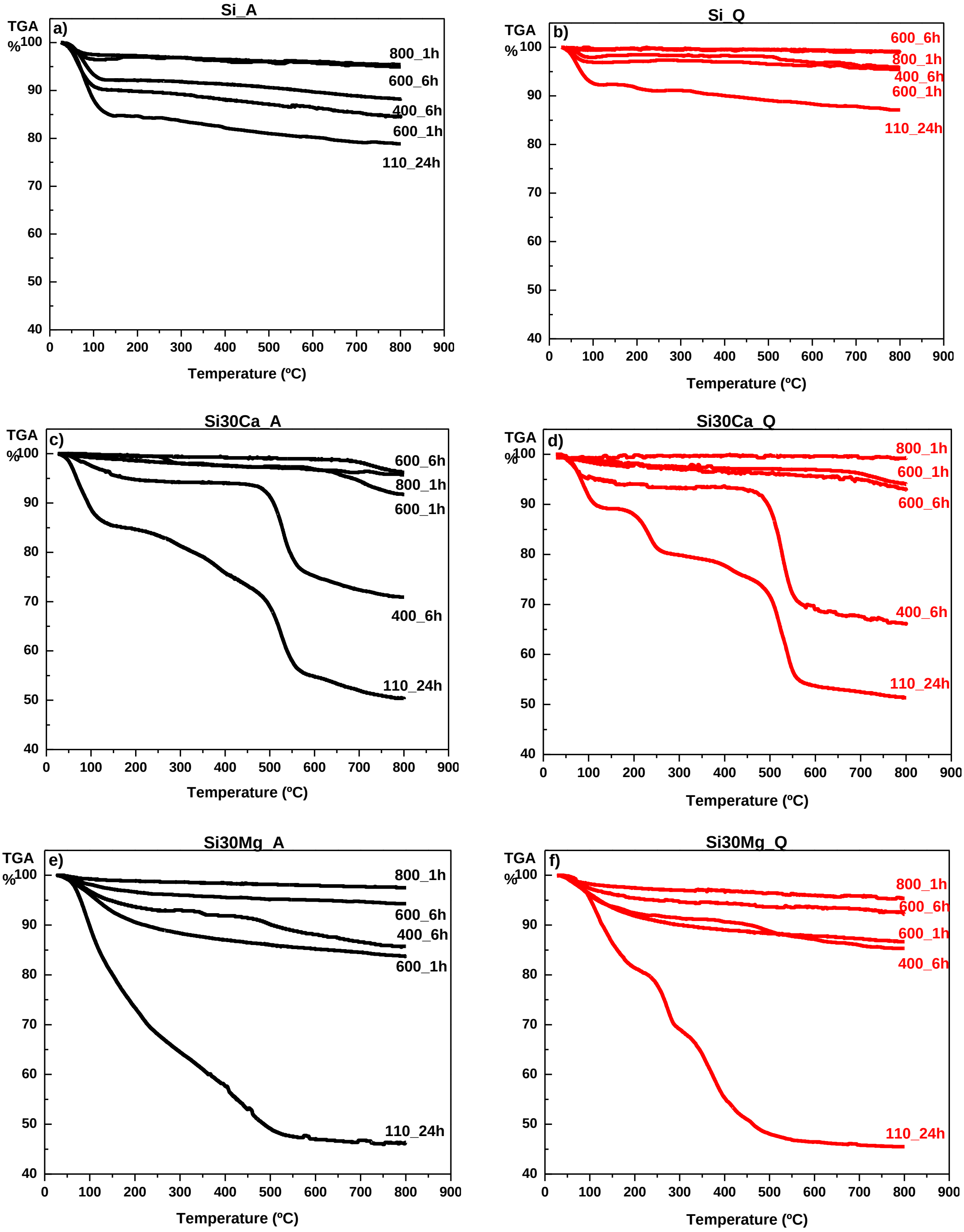

***Figure 2.7** TG results of the Si_A (a), Si_Q (b), Si30Ca_A (c), Si30Ca_Q (d), Si30Mg_A (e) and Si30Mg_Q (f) samples after various thermal treatments.*

The total weight losses of the Ca and Mg modified silicate glasses prepared by A and Q routes achieved after the calcination temperatures are presented separately for each sample in Figure 2.8. As revealed also from TG results it is clear that the solvent decomposition presents the higher mass loss and with increasing the heat treatment temperature the total weight loss decrease.

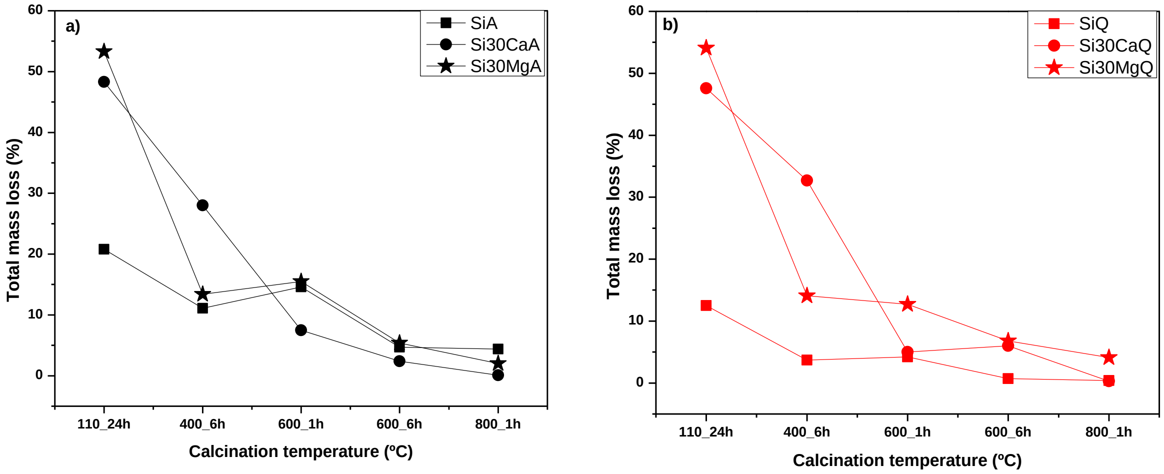

***Figure 2. 8*** *Total mass loss of the 100·$SiO_2$, 70·$SiO_2$·30·CaO, and 70·$SiO_2$·30·MgO samples prepare by A route (a) and by Q route (b) in function of calcination temperature.*

## 2.7 XRD measurements of thermal treated calcium silicate and magnesium silicate samples

X – Ray diffractograms were performed on the two component samples after they were heat treated at different temperatures for various length of time. The obtained results from the acid catalysed and quickly gelled glasses are presented in Figure 2.9.

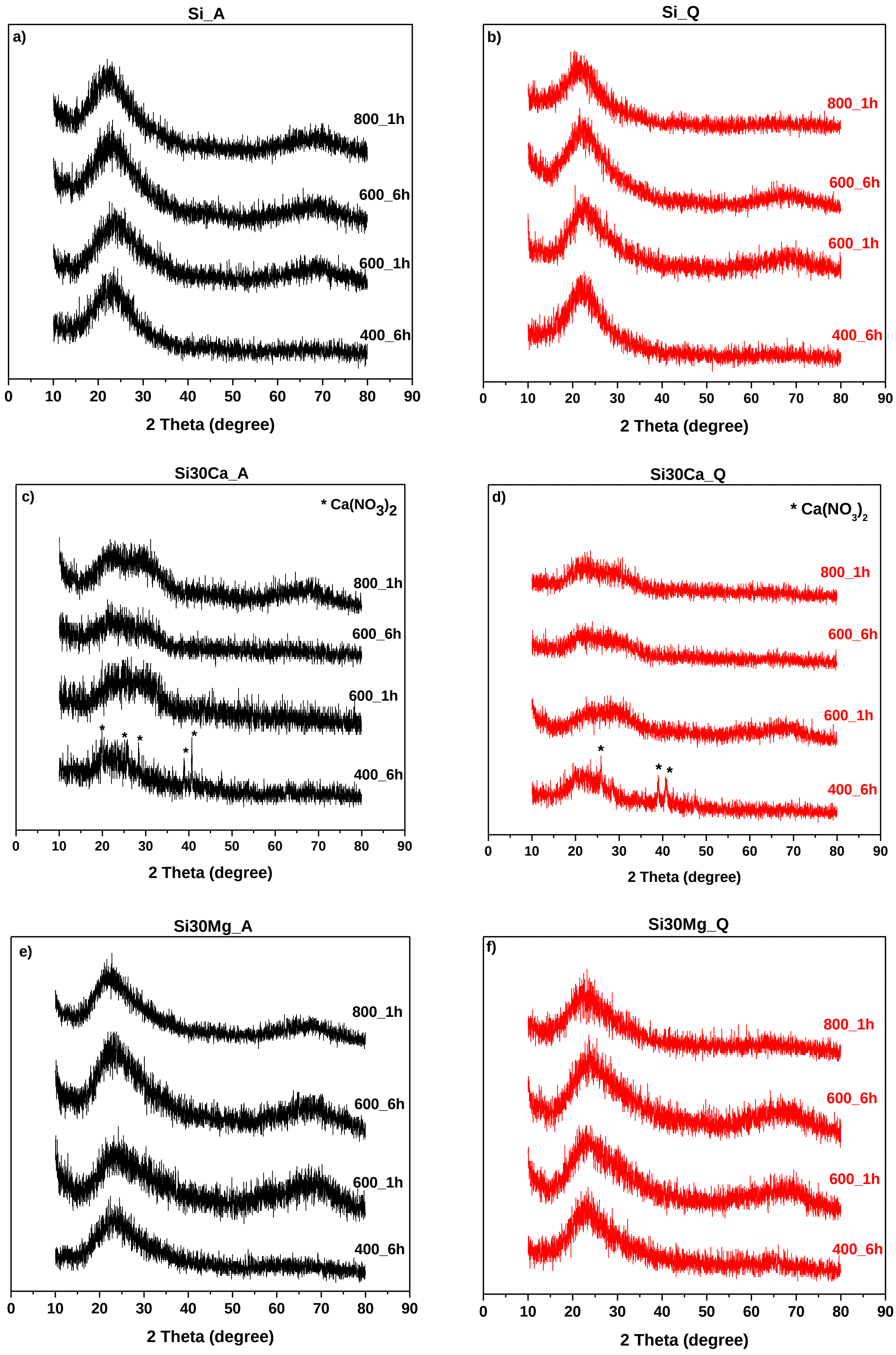

***Figure 2.9*** *XRD patterns of the 100·$SiO_2$, 70·$SiO_2$·30·CaO, and 70·$SiO_2$·30·MgO samples prepare by A route (a, c, e) and by Q route (b, d, f) after calcination temperatures.*

The XRD patterns reflect the amorphous nature of these samples with the large peak in 15- 35º interval in the 2θ degree even 800ºC_1h excepting the Si30Ca_A and Si30Ca_Q glasses heat treated at 400ºC_6h. The incipient crystalline phase at the calcium contained samples thermal treated at 400ºC_6h was identified as $Ca(NO_3)_2$ (calcium nitrate pdf No: 7-0204).

## 2.8 SSA measurements of thermal treated calcium silicate and magnesium silicate samples

BET surface area was measured after calcination of the studied samples at various temperatures for different length of times as shows Figure 2.10.

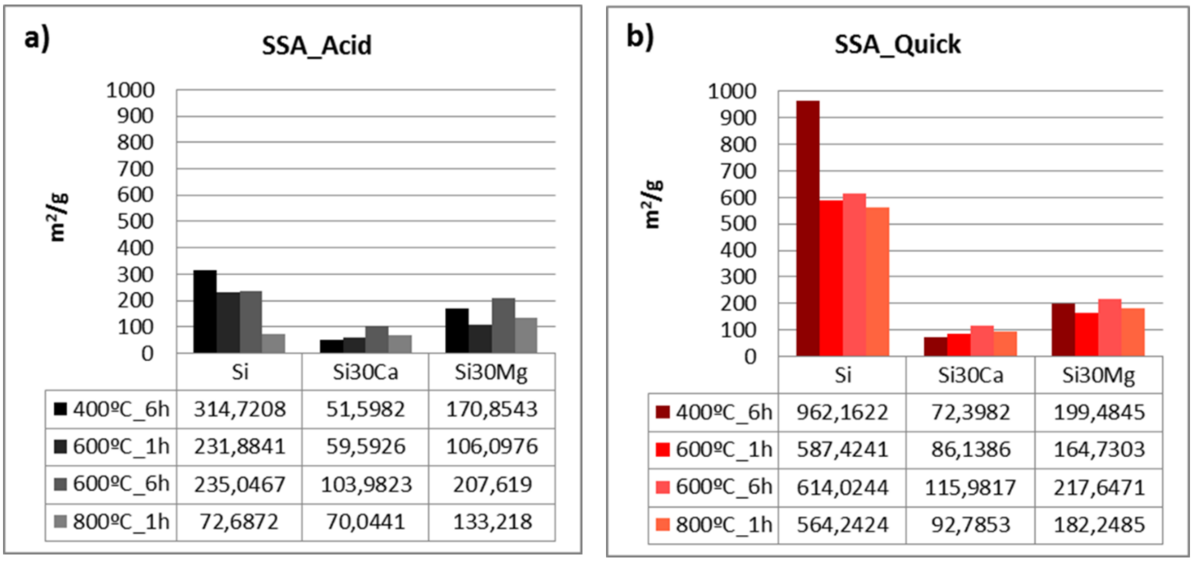

***Figure 2.10*** *Total surface area of the thermally treated samples for 400 ºC_6h, 600 ºC_1h, 600 ºC_6h and 800 ºC_1h obtained by A route (a) and by Q route (b).*

The highest values were obtained in case of the single component samples: Si_A and Si_Q. By increasing the calcination temperature until 600ºC_6h it can be remarked a gradual increase of the surface area of the two component samples and a sharp reduction at 800ºC _1h. The increase at lower temperatures may be due to the decomposition of nitrate and the remove of physically adsorbed water and residual organics stuck in the micro pores of the dried gels, supported also by DTA and TGA results. The decrease at 800ºC_1h may be attributed to an increase in the degree of cross-linking as the decomposition of silanols leads to polymerization or to glass network collapse.

## 2.9 FTIR spectroscopy of thermal treated calcium silicate and magnesium silicate samples

The relation between the microscopic structure and the IR vibrational modes of silicates has been the subject of intensive investigation also [20, 24]. The number of bands, their positions and shapes are almost identical for the two different gelled silica matrices as shows Figure 2.11 a) and b).

The band located at 465 $cm^{-1}$ is considered to become from the rocking motion of the bridging oxygen atoms perpendicularly to the Si–O–Si plane ($TO_1$). The second band at 805 $cm^{-1}$ can be assigned to the bending motion of the oxygen atom along the bisector of the Si–O–Si bridging group ($TO_2$), and the third high-energy band, at 1100 $cm^{-1}$, was attributed to the anti-symmetric stretching mode of Si–O–Si groups that involves mainly oxygen motion along the Si–Si direction ($TO_3$) [24]. The last vibration in this case is accompanied by the presence of an intense shoulder at the high frequency site ~1220 $cm^{-1}$ ($LO_3$) known as longitudinal-optic (LO) and transverse-optic (TO) splitting of the vibrational mode. While dealing with the IR-spectra of the silica samples, one important observation is the longitudinal-optic (LO) and transverse-optic (TO) splitting of the vibrational mode attributed to long range coupling of Columbic interactions arising due to the partial iconicity in the material [25]. Studies have revealed that the intensity of the $LO_3$ vibration mode increases with porosity in sol–gel derived glasses because of the scattering of the IR radiation within the pores and the consequent activation of the LO modes fact that is visible if comparing the acid prepared and the quickly gelled pure silica samples (Si_A and Si_Q).

The peak located at ~940 $cm^{-1}$ at A samples and at ~950 $cm^{-1}$ at Q samples is due to Si-OH bonds containing nonbridging oxygen and is attributed to mobile protons forming surface hydroxyl groups in aqueous process [26]. As the sintering temperature is increased, the absorption peak due to Si-OH bonds become weaker indicating that residual Si-OH polymerisation [30]. In the IR absorbance spectra of the two component sol–gel derived CaO (Figure 2.11 b, c) and MgO (Figure 2.11 d, e) -modified glasses can observe that the addition of alkaline earth oxide modifier causes significant spectral changes.

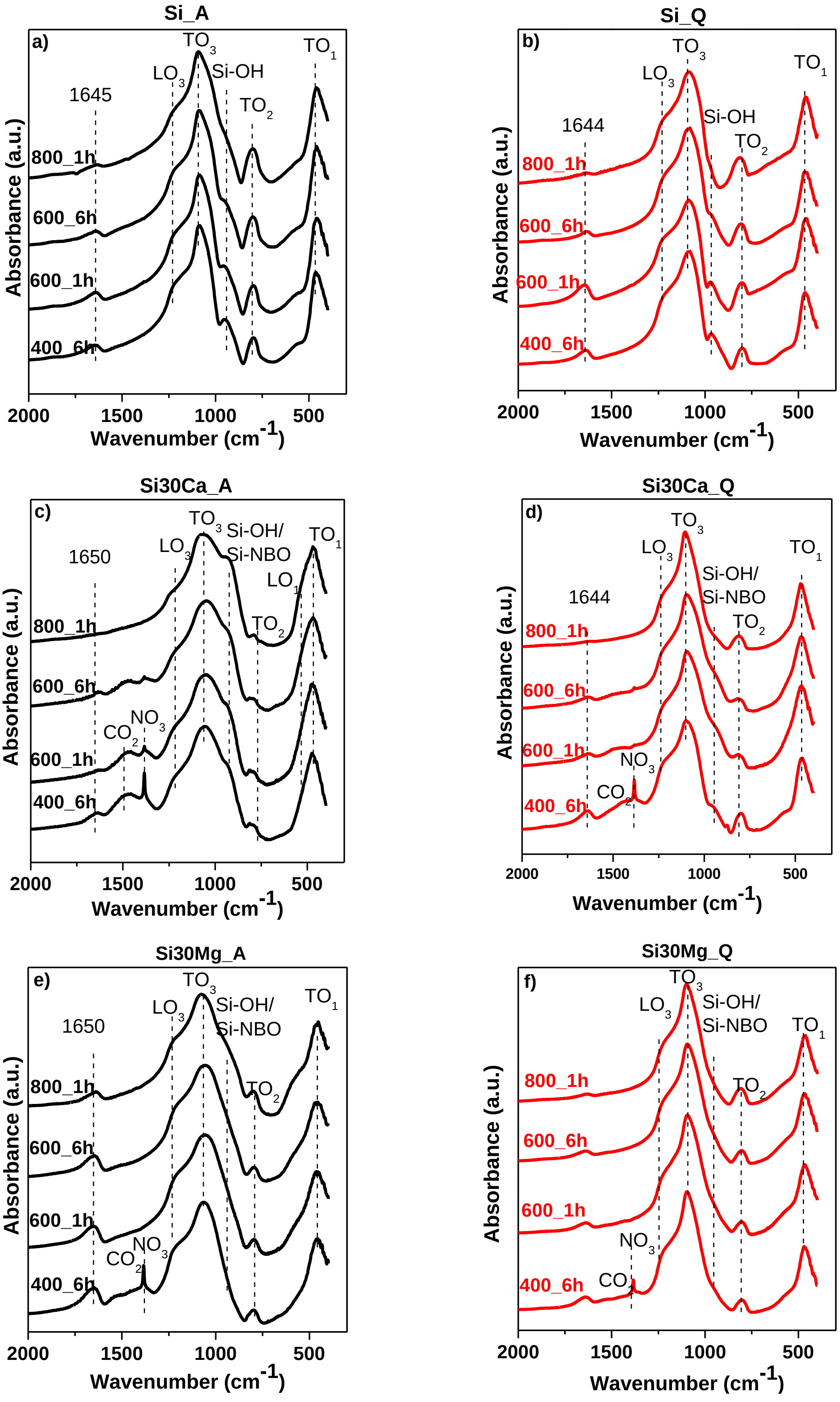

***Figure 2.11*** *FTIR spectra of the A and Q prepared 100·$SiO_2$ (a, b), 70·$SiO_2$·30·CaO (c, d), and 70·$SiO_2$·30·MgO (e, f) after thermal treatment of various temperatures.*

The changes are dependent also by the gelling time. In the low energy $TO_1$ mode there is a band widening towards higher wavenumber after alkaline earth oxide modifiers addition. This event is more evident for acid catalysed CaO-modified glasses. This enlargement could be associated with the $LO_1$ mode, which usually is inactive in IR spectrum of silica but can be activated in the case of strong distortion of the tetrahedral caused by high alkaline earth oxide content. The intensity of the bending mode at ~805 $cm^{-1}$ ($TO_2$) decreases with addition of calcium respectively magnesium oxide, the decrease in intensity being more dramatic in the $CaO–SiO_2$ systems then for $MgO–SiO_2$ glasses for both preparation methods. A new band at 930 $cm^{-1}$ develops at Si30Ca_A glass that may be attributed to Si-O-2NBO stretching vibration specific for silicate matrices with high modifier content [20, 27].

The thermal treatment temperature effect is visible on the bands located at around 1380 $cm^{-1}$, 1440 $cm^{-1}$ and 1645 $cm^{-1}$ peaks related to $(NO_3)^-$, $CO_3^{2-}$ and stretching vibration of H-O bonds respectively [28]. By increasing the temperature the nitrate decomposes, the carbonate are also eliminated, and the isolated OH intensity decrease [29].

Furthermore the shape of the vibration bands in 1000-1300 $cm^{-1}$ interval depends on preparation route. In case of the two components acid catalysed samples is broader than in the case of their quickly gelled counterparts. It has been reported that broad band is specific for high modifier presence in the silica network [27]. In our case the modifier content being the same in both preparation routs it means that the introduced alkaline earth oxides may behave as stronger modifiers in the A samples than in the Q gelled ones. The undetermined behaviour (modifier or intermediary) of magnesium oxide was previously reported [28], but calcium oxide is known as a consecrated network former.

The 600 ºC_6h treatment temperature proved to be the best, because thus obtained samples do not contain nitrate residues, present amorphous structure and have a higher surface area. Therefore all prepared samples from these sample set were stabilised at 600 °C for 6 hours and after that were subjected for *in vitro* testing.

### 2.10 Bioactivity studies

For *in vitro* investigation of the stabilised samples (Si_A, Si_Q, Si30Ca_A, Si30Ca_Q, SiCa10Mg_A, SiCa10Mg_Q, SiCa15Mg_A, SiCa15Mg_Q, SiCa20Mg_A, SiCa20Mg_Q, Si30Mg_A and Si30Mg_Q), 40 mg of each sample were immersed in 10 ml SBF at 37 °C under static conditions for 8 days. The SBF was renewed in the fourth day. Afterwards the immersed dried samples structure and morphological properties were investigated.

### 2.10.1 XRD measurements after SBF immersion

The structural properties of the thermal treated samples after SBF immersion were investigated by X-ray diffraction analysis and the obtained results are presented in Figure 2.12.

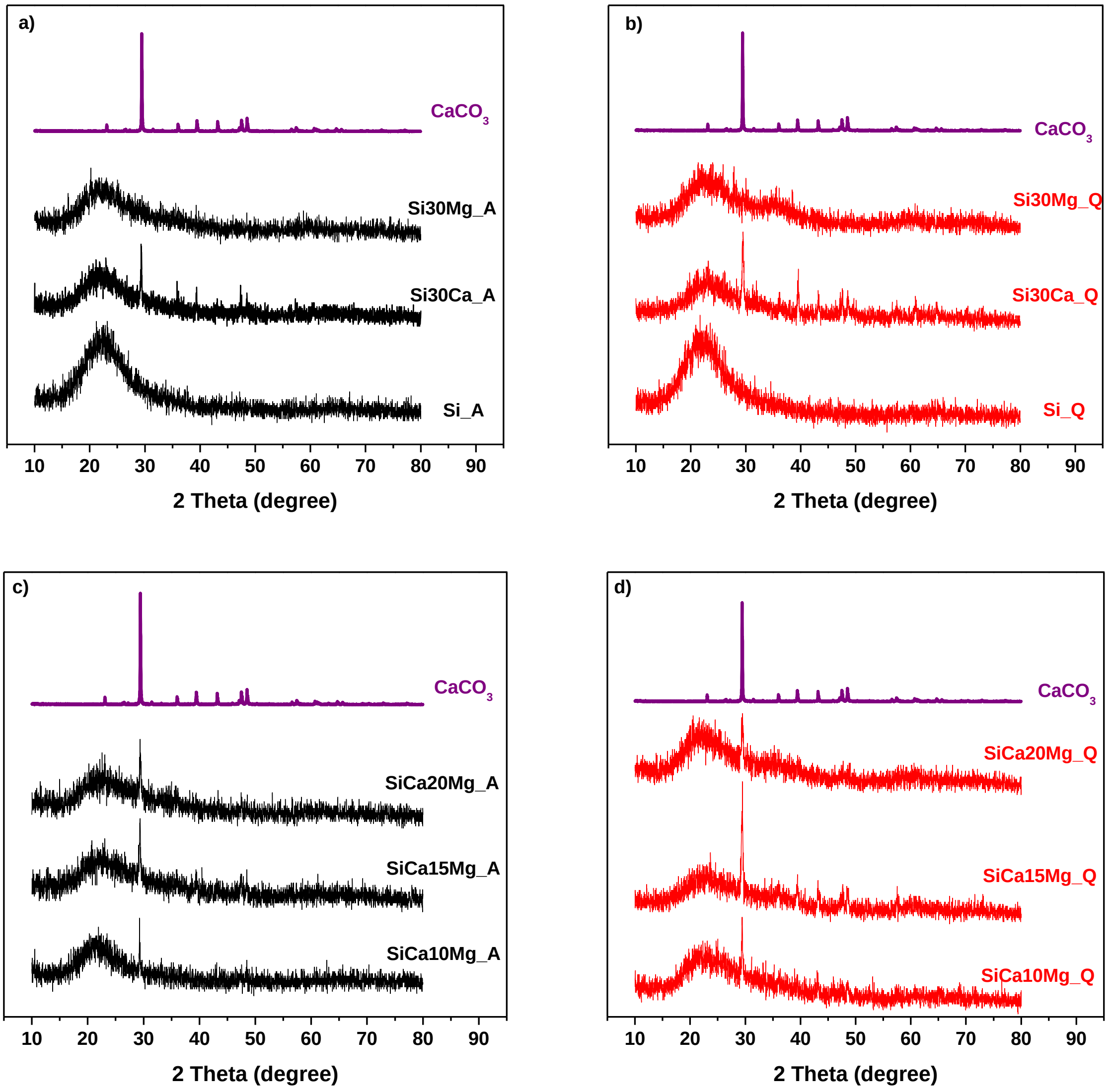

***Figure 2.12** XRD patterns of the Si, Si30Ca, Si30Mg A (a) and Q (b) prepared and SiCa10Mg, SiCa15Mg, SiCa20Mg A (c) and Q (d) prepared samples after SBF soaking for 8 days.*

Before incubation in SBF both acid catalysed (A) and quickly gelled (Q) sample sets present a predominant amorphous structure with a broad peak between 15-35 ° in the 2θ range. After immersion for 8 days on the samples surface developed calcium carbonate crystals as can be observed from XRD results, excepting Si and Si30Mg samples. The single component and the samples with maximum amount of magnesium prepared by sol- gel acid but also by quick gelation method inhibit the crystal growth on the sample surface.

### 2.10.2 FTIR measurements after SBF immersion

The structural properties of the thermal treated samples after SBF immersion were investigated also by FTIR spectroscopy and the obtained results are presented in Figure 2.13.

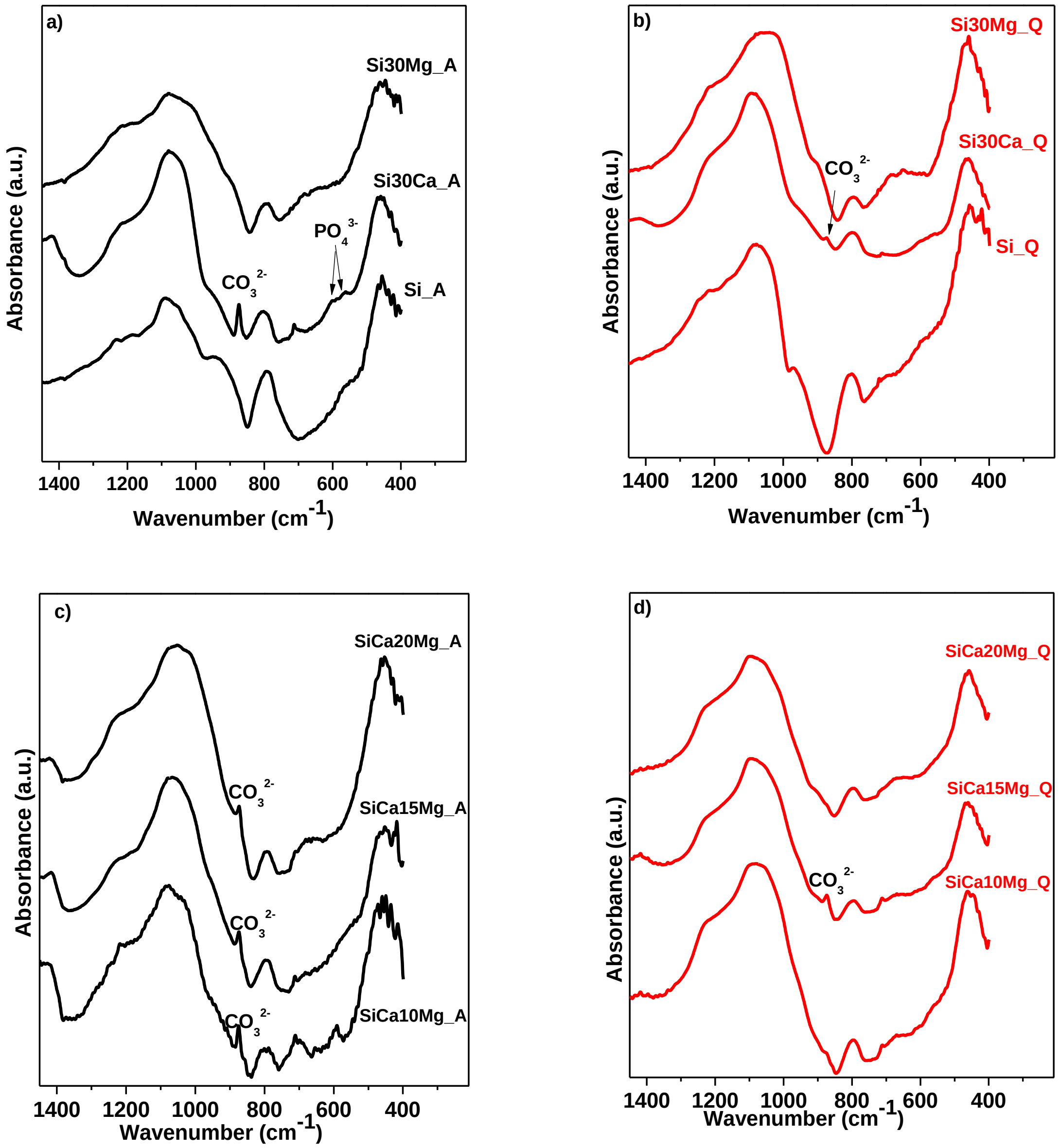

***Figure 2.13*** *FTIR spectra of the Si, Si30Ca, Si30Mg A (a) and Q (b) prepared and SiCa10Mg, SiCa15Mg, SiCa20Mg A (c) and Q (d) prepared samples after SBF immersion for 8 days.*

The presence of HA is visible just in case of Si30Ca_A with the appearance in the spectra of the absorption bands around 570 cm-$^{1}$ and 604 cm-$^{1}$, respectively, doublet characteristic for the vibration of $[PO_4]$ units from crystalline HA phase [34, 19]. The appearance of $[CO_3]$ vibration around 873 cm$^{-1}$ [30] in case of SiCa15Mg_Q, SiCa10Mg_A, SiCa15Mg_A, SiCa20Mg_A, Si30Ca_Q and Si30Ca_A samples indicate that after immersion of 8 days calcium carbonate developed on this samples surface.

### 2.10.3 SEM/ EDS measurements after SBF immersion

Scanning electron microscopy measurements and Energy dispersive X-ray spectroscopy analysis were also performed on the 8 days SBF soaked samples for morphological properties investigation (Figure 2.14).

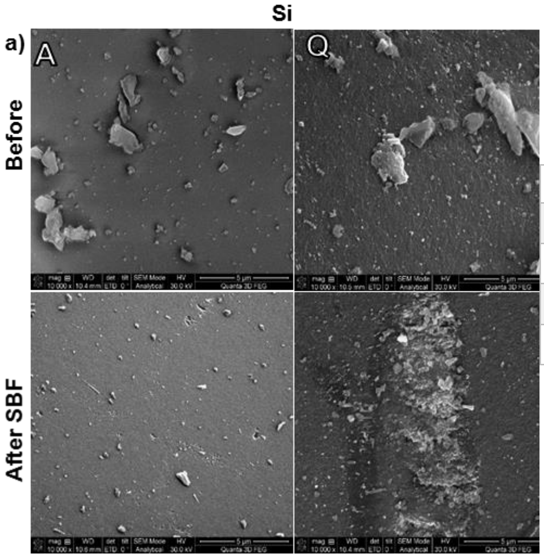

| | O | Si | Ca | P |
|---|---|---|---|---|
| **Si_A** | 61,76 | 38,24 | - | - |
| **Si_A_SBF** | 63,62 | 36,32 | 0,04 | 0,01 |
| **Si_Q** | 61,56 | 38,44 | - | - |
| **Si_Q_SBF** | 50,71 | 49,2 | 0,09 | - |

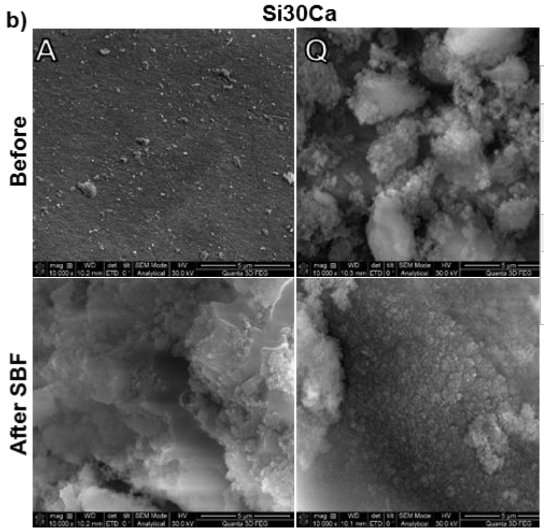

| | O | Si | Ca | P |
|---|---|---|---|---|
| **Si30Ca_A** | 45,84 | 38,99 | 15,17 | - |
| **Si30Ca_A SBF** | 55,33 | 2,69 | 35,97 | 6,02 |
| **Si30Ca_Q** | 50,65 | 31,61 | 17,74 | - |
| **Si30Ca_Q SBF** | 64,23 | 5,02 | 18,29 | 12,45 |

c)

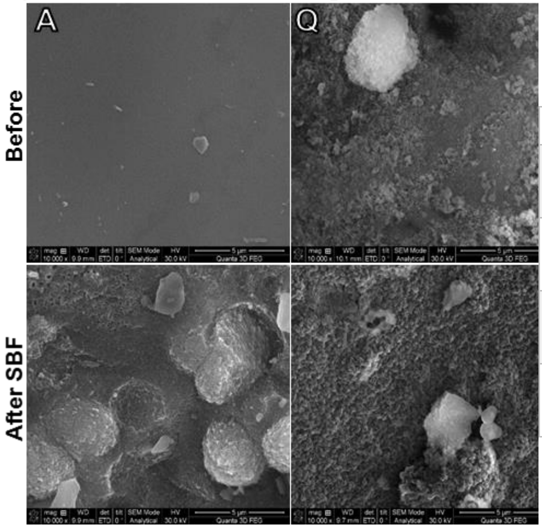

| | O | Si | Ca | P | Mg |
|---|---|---|---|---|---|
| **SiCa10Mg_A** | 56,32 | 35,17 | 4,27 | - | 4,27 |
| **SiCa10Mg_A SBF** | 57,24 | 34,44 | 4,39 | 3,76 | 0,17 |
| **SiCa10Mg_Q** | 56,55 | 32,59 | 6,9 | - | 3,96 |
| **SiCa10Mg_Q SBF** | 49,48 | 6,06 | 26,27 | 16,88 | 1,33 |

d)

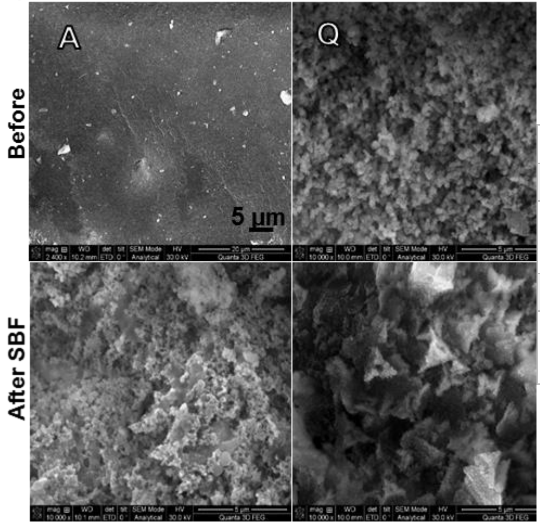

| | O | Si | Ca | P | Mg |
|---|---|---|---|---|---|
| **SiCa15Mg_A** | 51,94 | 37,34 | 3,98 | - | 6,73 |
| **SiCa15Mg_A SBF** | 54,27 | 32,42 | 2,9 | 3,6 | 6,81 |
| **SiCa15Mg_Q** | 51,33 | 36,53 | 8,15 | - | 3,99 |
| **SiCa15Mg_Q SBF** | 53,61 | 28,42 | 10,12 | 6,73 | 1,12 |

e)

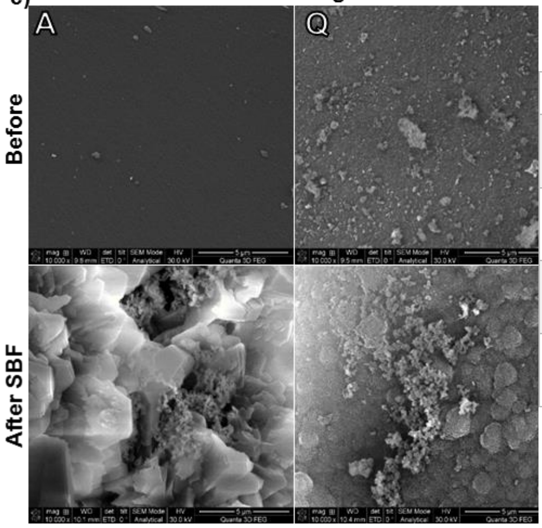

| | O | Si | Ca | P | Mg |
|---|---|---|---|---|---|
| **SiCa20Mg_A** | 50,24 | 32,92 | 7,88 | - | 8,97 |
| **SiCa20Mg_ASBF** | 53,54 | 24,42 | 9,49 | 2,56 | 9,99 |
| **SiCa20Mg_Q** | 40,64 | 36,86 | 10,85 | - | 11,64 |
| **SiCa20Mg_QSBF** | 60,33 | 30,73 | 2,69 | 2,88 | 3,37 |

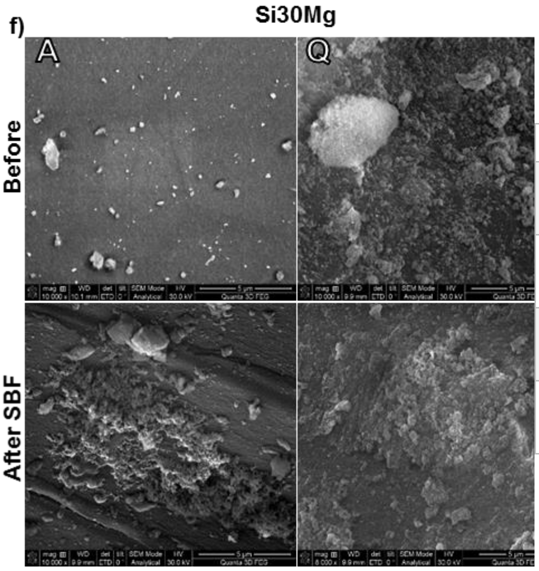

| | O | Si | Ca | P | Mg |
|---|---|---|---|---|---|
| **Si30Mg_A** | 49,16 | 35,54 | - | - | 15,29 |
| **Si30Mg_A SBF** | 57,07 | 34,15 | 0,56 | 1,1 | 7,12 |
| **Si30Mg_Q** | 56,84 | 28,19 | - | - | 14,97 |
| **Si30Mg_Q SBF** | 51,8 | 33,33 | 0,27 | 0,33 | 14,27 |

***Figure 2.14*** *SEM imagines and EDS diagrams from thermal treated at 600 °C for 6 hours A and Q prepared samples before and after SBF immersion. Scale bar correspond to 5 µm.*

The samples have different morphologies, and this depends on the chemical composition and the preparation route of the samples. The glasses prepared by Q route have a porous character in comparison with their A prepared counterparts. After immersion it can be observed changes on the sample surface, samples gelled quickly presents higher bioactivity. The magnesium together with calcium enhance the sample bioactivity under 15 % MgO concentration. Higher magnesium content as 15 % inhibit the hydroxyapatite formation.

Energy dispersive spectroscopy results (Figure 2.14 right column) supports the above mentioned bioactivity of the matrices, in case of quickly gelled samples the phosphor content is higher as at acid prepared once.

The majority of the obtained results were send for publication in specialized ISI journals.

## 2.11 Conclusions

Pure silica glass, and silicate glasses with CaO and MgO as glass network modifier with different magnesium content were synthesized via acid and quick sol-gel method.

According to the thermal history of the samples evaluated with DTA, a part from the prepared samples: Si_A, Si_Q, Si30Ca_A, Si30Ca_Q, Si30Mg_A and Si30Mg_Q, were heat treated at 400 ºC_6h, 600 ºC_1h, 600 ºC_6h and 800 ºC_1h for determining the optimal calcinations temperature. The FTIR spectra show that the 400 ºC calcination temperature demonstrated to be insufficient for the nitrate residues elimination, results supported by TGA where the weight loss are ~30% from the total mass, but is more efficient as the 600ºC_ 1h sintering temperature. XRD patterns highlight the 400 ºC treatment temperature inadequacy by calcium nitrate crystals appearance at SiCa samples, whereas the other samples have a preponderate amorphous structure. The 600 ºC_6h treatment temperature proved to be the best, because thus obtained samples do not contain nitrate residues demonstrated with DTA and TG, present amorphous structure confirmed by XRD, and have a higher surface area demonstrated by BET and confirmed by SEM measurements. It was sown that the Q method by rapid “frozen” of the network permits incorporation of high amount of modifiers as Ca or Mg oxide without destroying the silica network.

Characteristic quality for apatite and calcium carbonate phases were evidenced in XRD patterns and SEM/ EDS measurements recorded after all samples incubation in simulated body fluid for 8 days, but not for all the samples.

After immersion on the samples surface develops crystalline calcium carbonate and hydroxyapatite excepting Si_A, Si_Q and Si30Mg_A, Si30Mg_Q samples. Scanning electron microscopy measurements and energy dispersive ones supports the XRD results. In case of quickly gelled samples the phosphor content is higher as at acid prepared once, quick sol-gel preparation method enhance the bioactivity. Likewise magnesium inhibits the hydroxyapatite formation over 15 mol % of MgO. Samples containing CaO and MgO too are more bioactive under 15 % MgO concentration, so the SiCa10Mg_Q sample present a highest bioactivity from the prepared sample set.

## GENERAL CONCLUSIONS

- Silica glasses modified by CaO and MgO alkaline earth oxides ($SiO_2$, $SiO_2$-CaO, $SiO_2$-MgO and $SiO_2$-CaO-MgO) were successfully prepared via acid catalysed and quick acid catalysed base condensed sol-gel route.
- The 600 ºC_6h treatment proved to be the best, because thus we obtained samples which do not contain nitrate residues, present amorphous structure and have a high surface area.
- After the structural stabilisation process all quick acid catalysed base condensed sol-gel prepared samples have amorphous character and present higher porosity than their acid catalysed counterparts.
- The samples bioactivity tested in simulated body fluid is influenced both by the addition of alkaline earth oxides and by sol-gel preparation route.
- After 8 days of immersion on some samples surface develop crystalline calcium carbonate and hydroxyapatite excepting Si and Si-Mg samples. Ergo magnesium inhibits the hydroxyapatite formation over 15 mol % of MgO. Samples containing CaO and MgO too are more bioactive under 15 % MgO concentration, so the 10 % mol content of MgO prepared via quick set sol-gel route sample present the highest bioactivity among the prepared samples.
- The samples bioactivity was supported by self-assembly of an apatite phase after 14 days of immersion in SBF as evidenced by XRD and FTIR and supported by SEM and EDS analysis.
- The most bioactive of all the investigated samples are the samples prepared by quick acid catalysed base condensed sol-gel route containing both calcium and magnesium.
- Magnesium oxide was demonstrated to improve the bioactivity of glasses if prepared by alkali mediated sol-gel route, and to inhibit this property in case of acid catalysed route preparation.

## SELECTED REFERENCES

1. El-Gohary, M. I., et al. "Influence of composition on the in-vitro bioactivity of bioglass prepared by a quick alkali-mediated sol-gel method,”." Nature and Science 11.3 (2013): 26.
2. Balamurugan, A., et al. "Synthesis and characterisation of sol gel derived bioactive glass for biomedical applications." Materials Letters 60.29 (2006): 3752-3757.
3. Sepulveda, P., J. R. Jones, and L. L. Hench. "In vitro dissolution of melt-derived 45S5 and sol-gel derived 58S bioactive glasses." Journal of Biomedical materials research 61.2 (2002): 301-311.
4. Ma, J., et al. "In vitro degradability and bioactivity of mesoporous CaO-MgO-P2O5-SiO2 glasses synthesized by sol–gel method." Journal of sol-gel science and technology 54.1 (2010): 69-76.
5. Watts, S. J., et al. "Influence of magnesia on the structure and properties of bioactive glasses." Journal of Non-Crystalline Solids 356.9 (2010): 517-524.
6. Hesaraki, Saeed, Mojgan Safari, and Mohammad Ali Shokrgozar. "Composite bone substitute materials based on β-tricalcium phosphate and magnesium-containing sol–gel derived bioactive glass." Journal of Materials Science: Materials in Medicine 20.10 (2009): 2011-2017.
7. Staiger, Mark P., et al. "Magnesium and its alloys as orthopedic biomaterials: a review." Biomaterials 27.9 (2006): 1728-1734.
8. Brinker, C. J., & Scherer, G. W. (Eds.). (1990). Sol-gel science: the physics and chemistry of sol-gel processing. Gulf Professional Publishing.
9. Luz, Gisela M., and João F. Mano. "Preparation and characterization of bioactive glass nanoparticles prepared by sol–gel for biomedical applications." Nanotechnology 22.49 (2011): 494014.
10. Jones, W. M., and D. B. Fischbach. "Novel processing of silica hydrosols and gels." Journal of non-crystalline solids 101.1 (1988): 123-126.
11. Liu, X. Y., Ding, C. X., & Chu, P. K. (2005). Comparison in In Vitro Evaluation of Wollastonite and Dicalcium Silicate Coatings. Key Engineering Materials, 288, 359-362.
12. Innocenzi, P. (2003). Infrared spectroscopy of sol–gel derived silica-based films: a spectra-microstructure overview. Journal of Non-Crystalline Solids, 316(2), 309-319.
13. Kalampounias, A. G. (2011). IR and Raman spectroscopic studies of sol–gel derived alkaline-earth silicate glasses. Bulletin of Materials Science, 34(2), 299-303.
14. Lange, P. (1989). Evidence for disorder-induced vibrational mode coupling in thin amorphous SiO2 films. Journal of applied physics, 66(1), 201-204.
15. Serra, J., Gonzalez, P., Liste, S., Chiussi, S., Leon, B., Pérez-Amor, M., Ylänen, H. O., & Hupa, M. (2002) Influence of the non-bridging oxygen groups on the bioactivity of silicate glasses. J. Mater. Sci. - Mater. Med. 13(12), 1221-1225.
16. Watts, S. J., Hill, R. G., O’Donnell, M. D., & Law, R. V. (2010). Influence of magnesia on the structure and properties of bioactive glasses. Journal of Non-Crystalline Solids, 356(9), 517-524.
17. McMillan, P. W. (1979). Glass Ceramics, Academic Press, London.

18. Ma, J., Chen, C. Z., Wang, D. G., & Hu, J. H. (2011). Synthesis, characterization and in vitro bioactivity of magnesium-doped sol–gel glass and glass-ceramics. Ceramics International, 37(5), 1637-1644.
19. Kokubo, T. (Ed.). (2008). Bioceramics and their clinical applications. Elsevier.
20. Riti, P. I., Vulpoi, A., Ponta, O., & Simon, V. (2014). The effect of synthesis route and magnesium addition on structure and bioactivity of sol–gel derived calcium-silicate glasses. Ceramics International, 40(9), 14741-14748.
21. Xia, W., & Chang, J. (2007). Preparation and characterization of nano-bioactive-glasses (NBG) by a quick alkali-mediated sol–gel method. Materials letters, 61(14), 3251-3253.
22. López-Noriega, A., Arcos, D., Izquierdo-Barba, I., Sakamoto, Y., Terasaki, O., & Vallet-Regí, M. (2006). Ordered mesoporous bioactive glasses for bone tissue regeneration. Chemistry of materials, 18(13), 3137-3144.
23. Saravanapavan, P., & Hench, L. L. (2003). Mesoporous calcium silicate glasses. I. Synthesis. Journal of non-crystalline solids, 318(1), 1-13.
24. Chrissanthopoulos, A., Bouropoulos, N., & Yannopoulos, S. N. (2008). Vibrational spectroscopic and computational studies of sol–gel derived CaO–MgO–SiO2 binary and ternary bioactive glasses. Vibrational Spectroscopy, 48(1), 118-125.
25. De Leeuw, S. W., & Thorpe, M. F. (1986). Coulomb Splittings in Glasses.Physical Review Letters, 56(20), 2228.
26. Valliant, E. M., Turdean-Ionescu, C. A., Hanna, J. V., Smith, M. E., & Jones, J. R. (2012). Role of pH and temperature on silica network formation and calcium incorporation into sol–gel derived bioactive glasses. Journal of Materials Chemistry, 22(4), 1613-1619.
27. Serra, J., Gonzalez, P., Liste, S., Chiussi, S., Leon, B., Pérez-Amor, M., & Hupa, M. (2002). Influence of the non-bridging oxygen groups on the bioactivity of silicate glasses. Journal of Materials science: Materials in medicine, 13(12), 1221-1225.
28. Luz, G. M., & Mano, J. F. (2011). Preparation and characterization of bioactive glass nanoparticles prepared by sol–gel for biomedical applications. Nanotechnology, 22(49), 494014.
29. Bansal, N. P. (1988). Sol-Gel Synthesis of Magnesium Oxide-Silicon Dioxide Glass Compositions. Journal of the American Ceramic Society, 71(8), 666-672.
30. Nico, A. J. M., Ellen, N. M., & Matthijn, R. J. (2007). Calcium carbonate thin films as biomaterial coatings using DNA as crystallization inhibitor. CrystEngComm, 9(12), 1209-1214.

## ACKNOWLEDGEMENTS

First of all, I would like to thank all professors from Faculty of Physics of Babeș-Bolyai University, who imparted their knowledge since the first years of my studies.

I would like to express my deepest gratitude to the supervisor of my PhD thesis, Prof.dr. Viorica SIMON, for providing me the privilege to work in her research group. Her understanding, consideration, support and guidance have provided the basis for this thesis.

Moreover, I want to thank all my colleagues from the Institute for Interdisciplinary Research on Bio-Nano-Sciences, of Babeș- Bolyai University, for their help and useful discussions, especially to Dr. Adriana VULPOI for her advices and constructive critics and for mentoring me in the past three years.

I would like to express my love and gratitude to my parents, to my sister and my husband for their understanding, patience and permanent support, and for providing inspiration and energy during all these years.

Finally I acknowledge the financial support provided from programs co-financed by The Sectoral Operational Programme Human Resources Development, Contract **POSDRU/159/1.5/S/132400**.